

Journal Pre-proof

A systematic review of the molecular simulation of hybrid membranes for performance enhancements and contaminant removals

Cia Yin Yee, Lam Ghai Lim, Serene Sow Mun Lock, Norwahyu Jusoh, Chung Loong Yiin, Bridgid Lai Fui Chin, Yi Heng Chan, Adrian Chun Minh Loy, Muhammad Mubashir

PII: S0045-6535(22)02337-2

DOI: <https://doi.org/10.1016/j.chemosphere.2022.135844>

Reference: CHEM 135844

To appear in: *ECSN*

Received Date: 23 April 2022

Revised Date: 24 June 2022

Accepted Date: 22 July 2022

Please cite this article as: Yee, C.Y., Lim, L.G., Lock, S.S.M., Jusoh, N., Yiin, C.L., Chin, B.L.F., Chan, Y.H., Loy, A.C.M., Mubashir, M., A systematic review of the molecular simulation of hybrid membranes for performance enhancements and contaminant removals, *Chemosphere* (2022), doi: <https://doi.org/10.1016/j.chemosphere.2022.135844>.

This is a PDF file of an article that has undergone enhancements after acceptance, such as the addition of a cover page and metadata, and formatting for readability, but it is not yet the definitive version of record. This version will undergo additional copyediting, typesetting and review before it is published in its final form, but we are providing this version to give early visibility of the article. Please note that, during the production process, errors may be discovered which could affect the content, and all legal disclaimers that apply to the journal pertain.

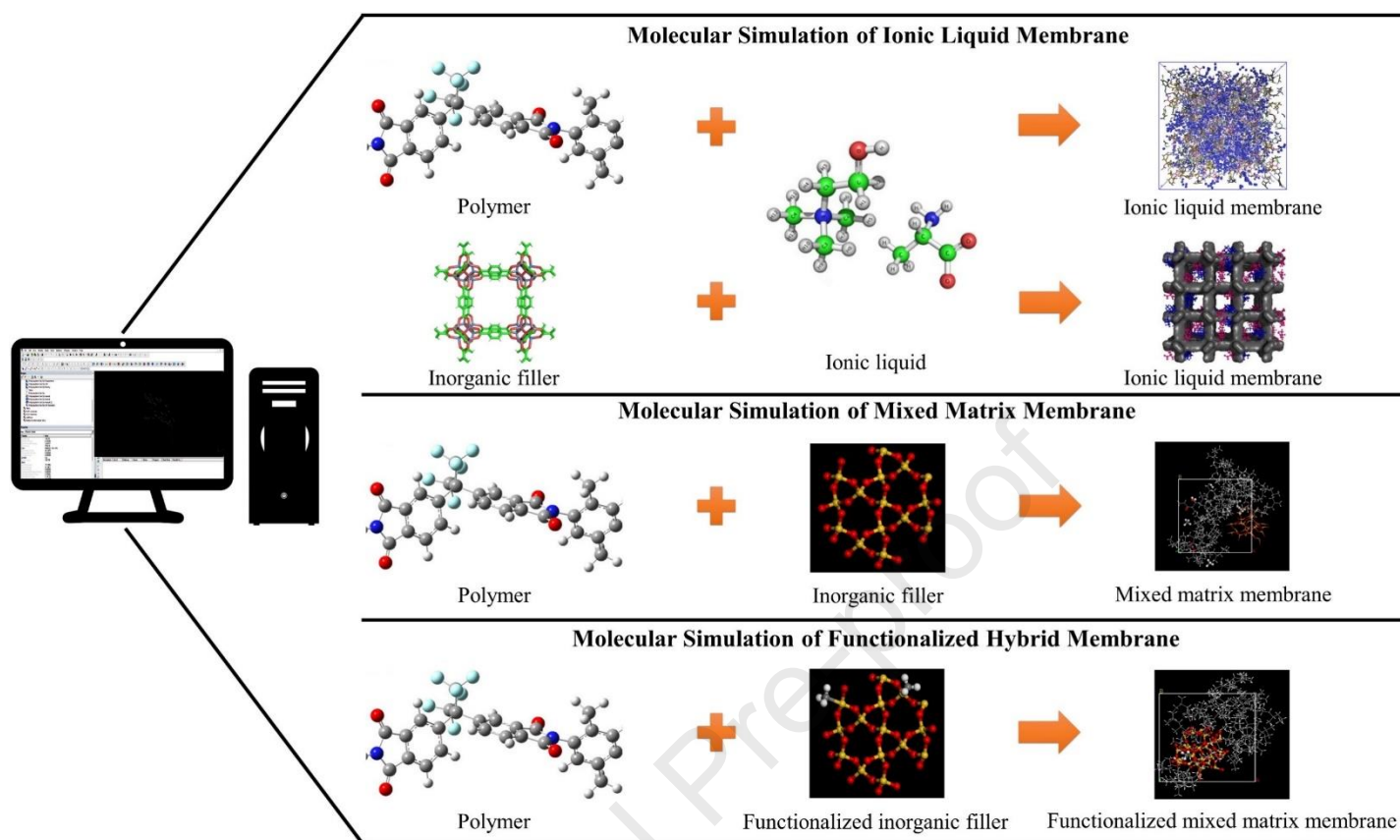
© 2022 Published by Elsevier Ltd.



Authorship Contribution Statement

Cia Yin Yee - Writing – Original draft; Data curation; Formal analysis; Investigation, Lam Ghai Lim - Formal analysis; Writing – review & editing; Investigation, Serene Sow Mun Lock – Formal analysis; Supervision; Writing – review & editing; Investigation, Norwahyu Jusoh – Resources; Writing – review & editing; Data curation, Chung Loong Yiin – Resources; Writing – review & editing; Data curation, Bridgid Lai Fui Chin – Resources; Writing – review & editing; Data curation, Yi Heng Chan – Resources; Writing – review & editing; Data curation, Adrian Chun Minh Loy – Resources; Writing – review & editing; Data curation, Muhammad Mubashir – Resources; Writing – review & editing; Data curation

GRAPHICAL ABSTRACT



A systematic review of the molecular simulation of hybrid membranes for performance enhancements and contaminant removals

Cia Yin Yee ^a, Lam Ghai Lim ^b, Serene Sow Mun Lock ^{a,*}, Norwahyu Jusoh ^a, Chung Loong Yiin ^{c,h}, Bridgid Lai Fui Chin ^d, Yi Heng Chan ^e, Adrian Chun Minh Loy ^f, Muhammad Mubashir ^g

^a *CO₂ Research Center (CO2RES), Department of Chemical Engineering, Universiti Teknologi PETRONAS, 32610 Seri Iskandar, Perak, Malaysia*

^b *School of Engineering, Monash University Malaysia, Selangor, Malaysia*

^c *Department of Chemical Engineering and Energy Sustainability, Faculty of Engineering, Universiti Malaysia Sarawak (UNIMAS), Kota Samarahan 94300, Malaysia*

^d *Department of Chemical Engineering, Faculty of Engineering and Science, Sarawak Campus, Curtin University Malaysia, Miri 98009, Malaysia*

^e *PETRONAS Research Sdn. Bhd. (PRSB), Lot 3288 & 3289, Off Jalan Ayer Itam, Kawasan Institusi Bangi, 43000 Kajang, Selangor, Malaysia*

^f *Department of Chemical Engineering, Monash University, Clayton, VIC 3800, Australia*

^g *Department of Petroleum Engineering, School of Engineering, Asia Pacific University of Technology and Innovation, 57000, Kuala Lumpur, Malaysia*

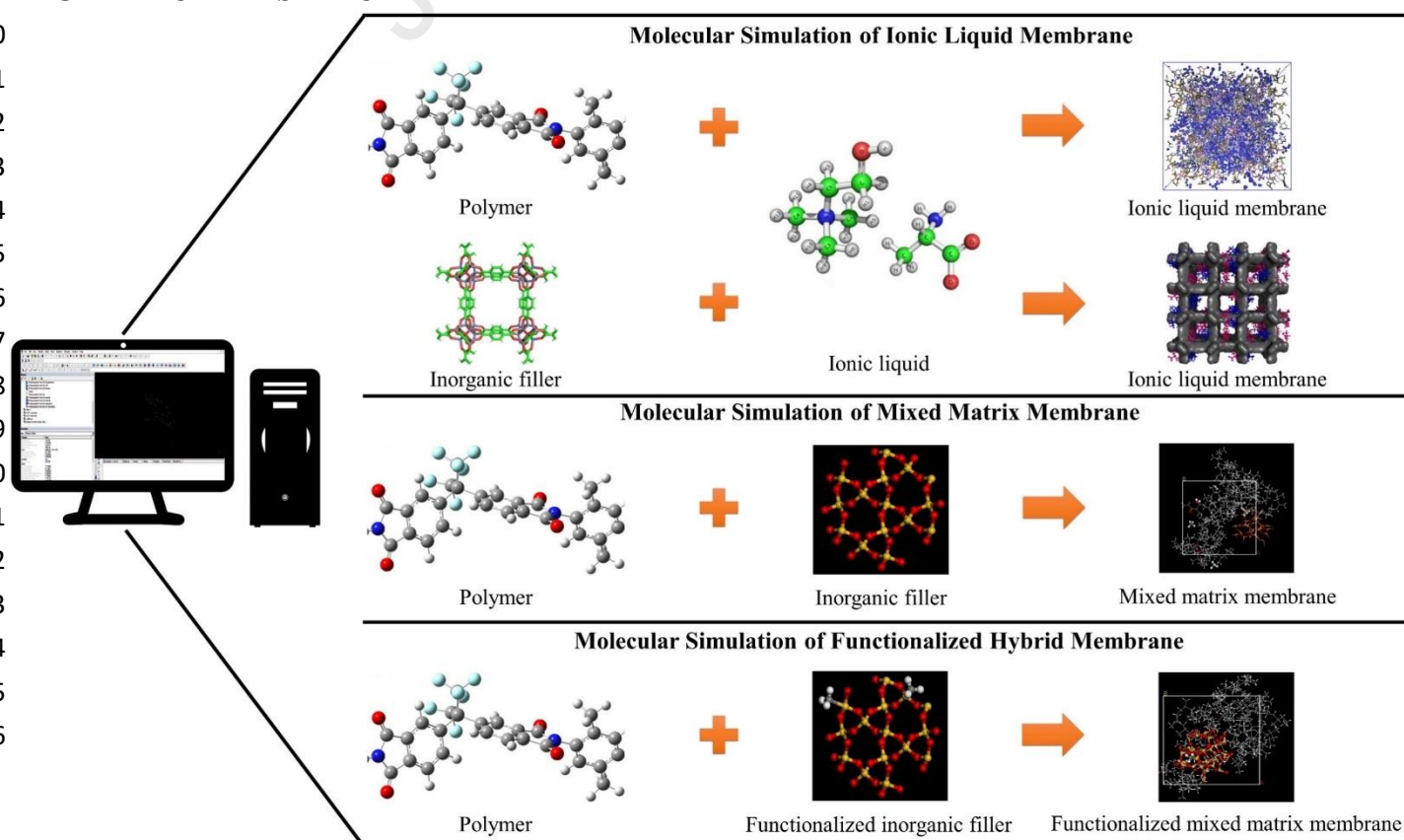
^h *Institute of Sustainable and Renewable Energy (ISuRE), Universiti Malaysia Sarawak (UNIMAS), 94300 Kota Samarahan, Sarawak, Malaysia.*

* Corresponding author. Department of Chemical Engineering, Universiti Teknologi PETRONAS, Bandar Seri Iskandar, 31750 Tronoh, Perak, Malaysia, Email address: sowmun.lock@utp.edu.my

HIGHLIGHTS

- Fundamentals of molecular simulation are reviewed and related to application in hybrid membranes.
- Insight into molecular structural properties of hybrid membranes is presented.
- Simulated transport performance from published literature and mechanism of hybrid membranes are provided.
- Limitation in molecular simulation for membrane separation is discussed.
- Future outlook for molecular simulation of membrane separation is recommended.

GRAPHICAL ABSTRACT



47 **AE**

48 Number of research on molecular simulation and design has emerged recently but there is currently a lack of review
49 to present these studies in an organized manner to highlight the advances and feasibility. This paper aims to review
50 the development, structural, physical properties and separation performance of hybrid membranes using molecular
51 simulation approach. The hybrid membranes under review include ionic liquid membrane, mixed matrix membrane,
52 and functionalized hybrid membrane for understanding of the transport mechanism of molecules through the different
53 structures. The understanding of molecular interactions, and alteration of pore sizes and transport channels at atomistic
54 level post incorporation of different components in hybrid membranes posing impact to the selective transport of
55 desired molecules are also covered. Incorporation of molecular simulation of hybrid membrane in related fields such
56 as carbon dioxide (CO₂) removal, wastewater treatment, and desalination are also reviewed. Despite the limitations
57 of current molecular simulation methodologies, i.e., not being able to simulate the membrane operation at the actual
58 macroscale in processing plants, it is still able to demonstrate promising results in capturing molecule behaviours of
59 penetrants and membranes at full atomic details with acceptable separation performance accuracy. From the review,
60 it was found that the best performing ionic liquid membrane, mixed matrix membrane and functionalized hybrid
61 membrane can enhance the performance of pristine membrane by 4 folds, 2.9 folds and 3.3 folds, respectively. The
62 future prospects of molecular simulation in hybrid membranes are also presented. This review could provide
63 understanding to the current advancement of molecular simulation approach in hybrid membranes separation. This
64 could also provide a guideline to apply molecular simulation in the related sectors.

65 **KEYWORDS:** Molecular simulation, membrane separation, ionic liquid membrane, mixed matrix membrane,
66 functionalized hybrid membrane

69 1. INTRODUCTION

70 In recent years, hybrid membranes have rapidly emerged as a promising technology to circumvent limitation in
71 polymeric membranes for separation process. Hybrid membranes have the advantage of combining two material
72 classes that can potentially modify the resultant structure, which outperform conventional membranes. High
73 selectivity and permeability that are superior to the Robeson plot have been achieved, along with durable and
74 optimized functions suited for specific applications. Different materials have been studied and reviewed for this
75 purpose, but they are mostly limited to state of art research using experimental approach. Recently, computational
76 chemistry has emerged as an indispensable tool to design new generation hybrid membranes with improved
77 separation performance. This enables minimization of intervention from costly and time-consuming experimental
78 method while providing insights at the atomic level, which is challenging or impossible to be measured using
79 laboratory instruments.

80 Molecular simulation is used to resolve the undiscovered aspects of a system, often much cheaper compared to
81 experiments (Mollahosseini and Abdelrasoul, 2021). Other advantages include the feasibility of designing different
82 simulation perspectives via manipulation of computational approaches. In addition, simulation assists in testing
83 conditions that are almost impossible at laboratory scales and reduces the handling of hazardous materials.

84 Investigation and analysis of the structural, physicochemical and transport behaviour of molecules through
85 varying types of materials with different system parameters can be accessible at the molecular or atomistic level.
86 The study variables may comprise glass transition temperature (T_g), pore size, fractional free volume, molecular
87 interaction, X-ray diffraction, solubility, sorption and diffusion mechanisms (Dehghani et al., 2017). This has
88 frequently found its application in estimation and calculation of various separation applications, which include gas
89 purification, biomedical engineering and wastewater treatment (Ebro et al., 2013; Hollingsworth and Dror, 2018;
90 An et al., 2019).

91 Alternatively, membrane system has an emerging role as a recognized eco-friendly separation process due to
92 its low energy consumptions in post-combustion carbon dioxide (CO_2) capture and storage, natural gas sweetening,
93 tertiary-level enhanced oil recovery, dehumidification, separation of acid gases, e.g., hydrogen sulphide (H_2S),
94 sewage treatment, desalination, and pharmaceutical (Brunetti et al., 2015; Le and Nunes, 2016; Vara et al., 2020).
95 In separation process utilizing membrane technology, membrane functions as a selective barrier to allow permeation
96 of one selective permeate while retaining other components (Zolghadr et al., 2021; Manikandan et al., 2022).
97 Permeability and selectivity are critical factors that affect the transport performance of membranes. Permeability of

98 porous membrane is affected by the permeate molecule size in which larger components have lower diffusion
99 coefficient and vice versa. On the other hand, permeability of non-porous membrane is influenced by the sorption
100 of penetrant molecules into the membrane, its diffusion through the membrane, and desorption at the downstream
101 of the membrane, which is known as the solution-diffusion mechanism (Freeman, 1999). Non-porous dense film
102 membranes transport solute through the pressure difference, concentration, or electric-field gradients on upstream
103 and downstream sides of the membrane (Rackley, 2017). Membrane selectivity is the ratio of permeability of the
104 relevant permeate and retentate passing through the membrane (Zolghadr et al., 2021).

105 The three core membrane materials used in various industries for separation purposes are organic (polymeric),
106 inorganic (graphene, carbon, zeolite, ceramic, metal, etc) and ionic liquid (He et al., 2018). Polymeric membrane
107 is robust and easy to fabricate, but it has disadvantages of lower performance due to its inherent permeability-
108 selectivity trade-off (Wu et al., 2020) (Freeman, 1999; Wong and Jawad, 2019). Substantial efforts have been
109 ongoing to improve permeability and selectivity of organic membranes to increase its commercial competitiveness.
110 On the other hand, inorganic membranes have excellent permeability, but their fabrication costs are generally higher
111 (Jusoh et al., 2016). Ionic liquids (ILs) are salts made through association of large organic cations with a wide
112 variety of anions, which offer high flexibility in designing new generation advanced materials for contaminant
113 removal (Swati et al., 2021). ILs also inherit downsides, which include high viscosity, high cost, toxicity in abundant
114 amount, which hinder their further expansion in industrial application.

115 A combination of the aforementioned materials is known as hybrid membrane. Hybrid membranes, a
116 breakthrough of membrane technology, integrating the advantages of polymeric or inorganic or ionic liquid
117 materials together (Jusoh et al., 2016). Hybrid membrane may be a solution to improve and modify the intrinsic
118 property of the pristine material in a less costly manner and to be engineered to a specific use. Some of the crucial
119 parameters for designing an efficient hybrid membrane include the selection of materials for the polymer, inorganic
120 filler and ionic liquid, the composition of the selected materials, and operating conditions (Singh, 2005; Liguori and
121 Wilcox, 2018; Gokulakrishnan et al., 2021).

122 Acting as an experiment guide, molecular simulation tool can be used to provide atomistic understanding and
123 characterization of the tailor-made combination of membrane materials, its individual polymer, filler and ionic
124 liquid (Keskin and Alsoy Altinkaya, 2019). Currently, comprehensive study of molecular structure of hybrid
125 membranes and their separation mechanism is limited. This may be due to the reason that hybrid membranes are
126 still mainly applied in laboratory settings and have yet to be widely applied in industry (Golzar et al., 2017a). The

127 excellent separation performance reported in laboratory studies may pave the way for hybrid membranes to expand
 128 its use in industry but further elucidation from molecular simulation is required.

129 In this paper, a systematic review of the recent advances in membrane development for gas separation, water
 130 desalination, and wastewater treatment are presented. This includes the basic principles of different membrane
 131 processes using molecular simulation, such as ionic liquid membrane (ILM), mixed matrix membrane (MMM), and
 132 functionalized hybrid membrane (FHM). Subsequently, recent studies on membrane advances in various
 133 applications are reviewed. Lastly, future perspectives on the development of membrane separation using molecular
 134 simulation technique are provided.

135 2. MOLECULAR SIMULATION AND APPLICATION IN MEMBRANE SEPARATION

136 The advancement and development of membrane appliances and its application software have demonstrated the
 137 importance of molecular simulation in understanding, predicting, and validating structure-property relationship of
 138 various membranes. In general, molecular simulation works by performing atomistic simulation to elucidate the
 139 system evolution, which is majorly based on 1) molecular dynamics (MD) that is a time-dependent evolution of the
 140 system and 2) Monte Carlo (MC) simulation that involves randomly sampling of the energy landscape to determine
 141 the probability with least value. The fundamentals, principals and functionalities underlying molecular simulation
 142 and relationship with membrane system is discussed in this section.

143 2.1 Fundamentals in Molecular Simulation

144 Molecular simulation aims to replicate properties of a macroscopic (bulk) system using atomistic calculation.
 145 However, the largest computers can only simulate systems with about 10^6 atoms, but a realistic macroscopic system
 146 has an order of 10^{23} atoms (Alavi, 2020). Thus, periodic boundary conditions are applied to overcome the limitation
 147 of molecule numbers in simulations (Shirts et al., 2006; Sharma, 2019). This solves the problem of finite simulation
 148 size and removes the surface effects. A crucial factor in MD simulation is the energy function that quantifies the
 149 intermolecular or/and intramolecular forces since it determines the simulation speed and accuracy. The energy is
 150 often computed based on a force field that defines the atomic bond strength and relationship between atoms in the
 151 same molecule and those in others, as shown in Eq. (1).

$$152 E_{total} = E_{bond}(r) + E_{angle}(\theta) + E_{dihedral}(\phi) \\
 153 + E_{non-bonding}(r) + E_{electrostatic}(r) \quad \text{Eq. (1)}$$

154 In the energy term, total energy of the system, E_{total} , is characterized by the bonded energy and the non-bonded
 155 energy contributions. The bonded energy is consisted of (i) the covalent bond stretching energy terms, $E_{bond}(r)$ (ii)
 156 the bond angle bending energy terms, $E_{angle}(\theta)$ and (iii) the torsion angle rotation energy terms, $E_{dihedral}(\phi)$ while

157 the non-bonded energy is described by van der Waals interaction $E_{\text{van der Waals}}(r)$ and electrostatic force
 158 $E_{\text{electrostatic}}(r)$ (Lock et al., 2018). The parametrized terms used in force field for energy computation are obtained
 159 by fitting with experimental work and mechanical quantum studies from small molecules (Adcock and McCammon,
 160 2006).

161 In classical MD, the atomic and molecular structures and interactions influence the velocities and positions of
 162 the molecules according to Newton's equation of motion. The length is measured in nanoscale and the time, t , is
 163 measured in nanoseconds in classical mechanical microscopic description (Cai et al., 2012; Alavi, 2020). Eq. (2)
 164 and Eq. (3) describe the aforementioned laws in a basic molecular simulation (Hernández-Rodríguez et al., 2016;
 165 Alavi, 2020; Moqadam et al., 2021):

$$166 \quad F_i = m_i a_i = m_i \frac{d^2 r_i}{dt^2} \quad \text{Eq. (2)}$$

$$167 \quad F_i = -\nabla_i U(r_i) = \frac{\partial U(r^N)}{\partial r_i} \quad \text{Eq. (3)}$$

168 where m , r , and U represent the mass of the molecule, the distance between two atoms or molecules, and the potential
 169 energy. MD propagates the coordinates and velocities of molecules in time to solve Newton's equations of motion
 170 (Jiang et al., 2020). Valid initial conditions of the systems and methods, e.g., the nature of boundary conditions
 171 confining the molecules and the inter- and/or intra-molecular interactions, need to be applied beforehand (Alavi,
 172 2020). Maxwell-Boltzmann distribution is applied to assign the initial velocities of the molecules at the simulation
 173 temperature. The momentum, p , and position, q , of a complicated system is described in Eq. (4) and Eq. (5)
 174 (Mollahosseini and Abdelrasoul, 2021).

$$175 \quad q(t + \Delta t) = q(t) + \frac{q(t)}{m} \Delta t \quad \text{Eq. (4)}$$

$$176 \quad p(t + \Delta t) = p(t) + ma(t)\Delta t \quad \text{Eq. (5)}$$

177 where $a(t)$ is the acceleration as a function of time.

178 With regards to the initial density during MD in search of the equilibrated structure, measured experimental value
 179 especially in the liquid phase can be used as the starting condition. The volumes, molecular position, orientation
 180 and energy in the system are varied in isothermal-isobaric (constant N, P, T) MD simulations, the initial density will
 181 differ during the simulation. Therefore, the resulting and equilibrated density is only known after completing the
 182 computation.

183 After achieving equilibration state from MD, the general physical properties A under canonical ensemble
 184 (constant N, V, T) can be calculated using Eq. (6) (Mollahosseini and Abdelrasoul, 2021).

$$185 \quad A = \iint A(q, p) P(q, p) dp dq \quad \text{Eq. (6)}$$

186 where $A(\rho, n)$ is the physical property of equilibrium state and $D(\rho, n)$ is the probability function of atoms arranged
187 in a molecule.

188 On the other hand, the MC algorithms operate based on equilibrium statistical mechanics for prediction of
189 probability of varying outcomes via translation, displacement, rotations of molecules or insertion and deletion of
190 sorbates on a simulation cell. Acceptance probability is used to govern configuration of the new structure from the
191 previous state. Example of the probability distribution for a system with N molecules under a MC isothermal-
192 isobaric condition is given in Eq. (7) (Corti, 2002).

$$193 \quad P(\{\rho\}, V; T, P) = \frac{V^N}{N! \Lambda^{3N}} e^{PV/kT} e^{-U(\{\rho\}; N, V)/kT} \quad \text{Eq. (7)}$$

194 where N is number of molecules, P is pressure, T is temperature, ρ is density, V is the volume, U is the potential
195 energy, k is a gas constant.

196 2.2 Fundamental Approaches Employed in Membrane Simulation

197 The mean square displacement MSD calculates the displacement of particle through the membrane via the MD
198 approach (Bouزيد et al., 2018), as shown in Eq. (8).

$$199 \quad MSD_i = \frac{1}{N} \sum_{i=1}^n \{|r_i(t) - r_i(0)|^2\} \text{disrupt} \quad \text{Eq. (8)}$$

200 The diffusion coefficient D is calculated through tracking of the gas molecule displacement via the Einstein self-
201 diffusion correlation (Einstein and Schilpp, 1979) as depicted in (9).

$$202 \quad D_i = \frac{1}{6N} \lim_{t \rightarrow \infty} \frac{d}{dt} \sum_{t=1}^N \langle |r_i(t)^2 - r_i(0)^2| \rangle \quad \text{Eq. (9)}$$

203 In Eq. (8) and Eq. (9), N represents the total number of diffusing atoms i within the hypothetical cell under
204 consideration, r_i is the position vector of atom i , $|r_i(t)^2 - r_i(0)^2|$ represents ensemble averages of the gas particles
205 MSD, while $r_i(t)$ and $r_i(0)$ depicts the final and initial position vector of the centre of mass of gas molecule over
206 the time span of interest, t .

207 From MC simulation, the sorption of molecules or ions within the membrane cell of interest can be simulated
208 under different ensembles, which include 1) canonical ensemble to find the preferred locations and energies given
209 a number of sorbates 2) grand canonical (GCMC) ensemble to predict the number of sorbates under fixed simulation
210 temperature and pressure and 3) uniform ensemble to compute the limit of loading of sorbate at low pressure limit
211 in order to know the Henry constant. The solubility coefficient of species i can be found through gradient of the
212 straight line connecting a point on the solubility isotherm to the origin using GCMC method.

$$213 \quad S_i = \lim_{f_i \rightarrow 0} \left(\frac{C_i}{f_i} \right) \quad \text{Eq. (10)}$$

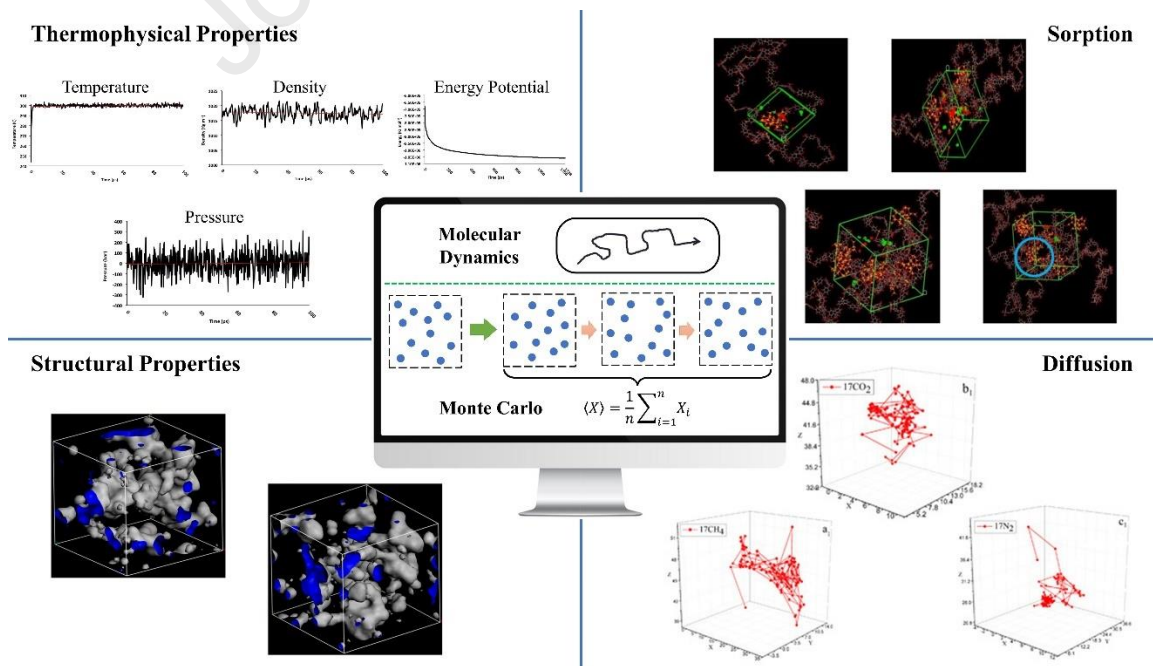
215 Fickian law of diffusion explains the fundamental for all transport phenomenon. The flux, J_i , defines the
 216 number of molecules for gas component i that penetrates through a unit area of unit time is directly proportional to
 217 the concentration gradient from the region of high to low end, $\frac{dc_i}{dx}$, through the diffusion coefficient, D_i , as depicted
 218 in Eq. (11).

219
$$J_i = -D_i \frac{dc_i}{dx} \quad \text{Eq. (11)}$$

220 Radial distribution function (RDF) also discloses conditions and methods of non-bonding interaction between
 221 molecules and the density change at a distance from a specific particle (McCarthy and Vaughan, 2015). It is a
 222 probability of finding a particle at a radial distance r from another particle in a random distribution that serves as
 223 the centre of reference (Rindt and Gastra-Nedeia, 2015).

224
$$g_{M-i}(r) = \frac{1}{\rho_{M-i} 4\pi r^2} \frac{\sum_{t=1}^K \sum_{j=1}^{N_{M-i}} \Delta N_{M-i}(r \rightarrow r + \delta r)}{N_{M-i} \times K} \quad \text{Eq. (12)}$$

225 $g_{M-i}(r)$ is the RDF, N_{M-i} is the total number of membrane molecules, M , and gas species i in the system, K the
 226 number of time steps, δr the distance interval, ΔN_{M-i} the number of gas i (or M) molecules between $r + \delta r$ around
 227 a M (or gas i) molecule, and ρ_{M-i} the bulk density of membrane system with presence of gas. RDF of gas i around
 228 functional groups of the membrane unit can be investigated. Figure 1 summarizes of the fundamentals in molecular
 229 simulation.



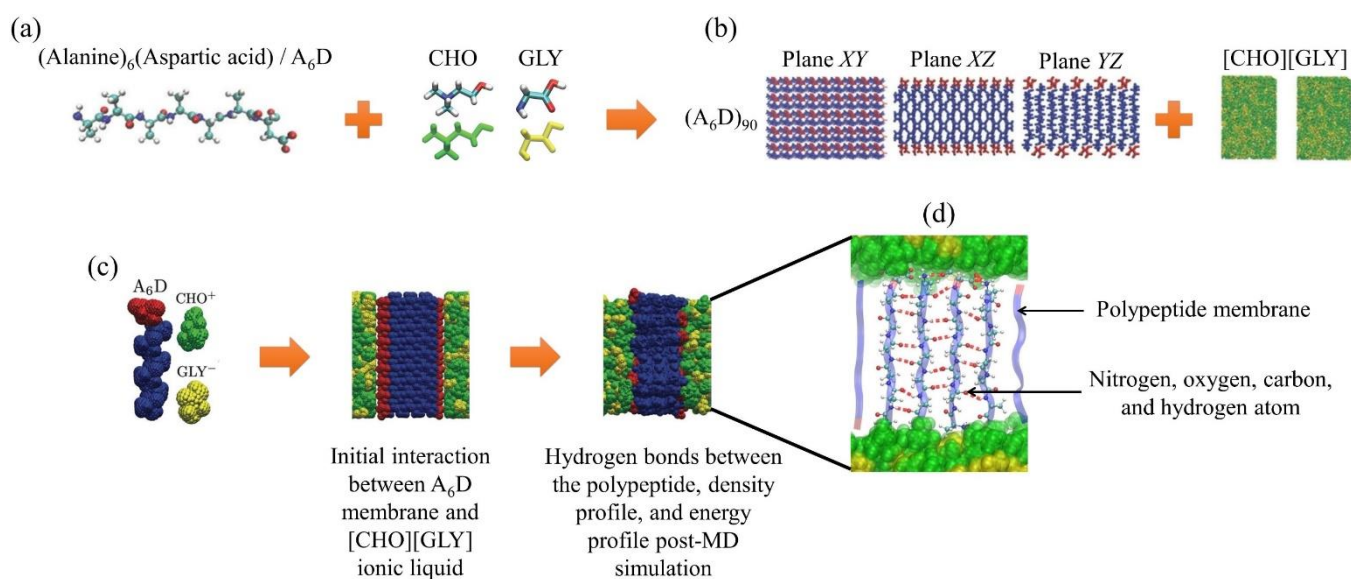
230

231 **Fig. 1** Fundamentals of molecular simulation including Molecular Dynamics and Monte Carlo simulations

233 Molecular simulations can be used to demonstrate the adsorption ability, permeability, and selectivity of hybrid
 234 membranes. It shows great potential to predetermine the capability, practicality, and functionality of the membrane
 235 before proceeding with the actual synthesis of the costly membranes. This section discusses the computation of
 236 ILM, MMM and FHM.

237 3.1 Ionic Liquid Membrane

238 Two main method of using ionic liquids in membrane materials are supported ionic liquid membrane (SILM)
 239 and quasi-solidified ionic liquid membrane (QSILM) (Wang et al., 2016b). SILM consists of a thin microporous
 240 support with ionic liquid filled pores (Wang et al., 2016b). QSILM is prepared by casting ionic liquid solution and
 241 a special gel to form a thin and stable quasi-solidification film (Wang et al., 2016b). Quasi-solidification of ionic
 242 liquid is a reliable way to prevent leakage by the self-assemble of organic molecules as compared to SILM (Wang
 243 et al., 2016b). Modelling ILM via molecular simulation aids in capturing the chemical structure stability at small
 244 step size modifications, which is not feasible in experiments. Molecular study of ILM along with its application and
 245 computed transport performance are provided in Table 1. Figure 2 shows the molecular dynamics simulation for
 246 ILM and the structural behaviour of the system, hydrogen bonds between the polypeptide membrane and IL, IL
 247 mobility, nanosheet energetic behaviour, and membrane surface topology. Figure 2 (a) discussed the initial structure
 248 of A_6D polypeptide membrane molecules and $[CHO][GLY]$ ionic liquids while Figure 2(b) shows the equilibrated
 249 structure of the superficial and lateral view of A_6D membrane nanosheet and $[CHO][GLY]$. Figure 2(c) and (d)
 250 illustrates the interactions between A_6D molecules and $[CHO][GLY]$ ionic liquids and A_6D nanosheet structure with
 251 hydrogen bonds formed between polypeptides, respectively.



252
 253

254 **Fig. 2** Molecular simulation studies of the structural behaviour of ILM. (a) Simulated initial structure A_6D
 255 polypeptide membrane molecules and $[CHO][GLY]$ ionic liquids. (b) Simulated equilibrated structure of the

256 superficial and lateral view of A₆D membrane nanosheet and [CHO][GLY] A = alanine (blue), D = aspartic acid
257 and
258 [CHO][GLY] ionic liquids. (d) A₆D nanosheet structure with hydrogen bonds (red dotted lines) formed between
259 polypeptides. Nitrogen, oxygen carbon, and hydrogen are shown in blue, red, cyan, and white colours. Ionic liquid
260 is in green-yellow colour. The molecular interactions between polypeptides are displayed in red-blue ribbon
261 representation. Figures are adapted from Ref. (Alves et al., 2019).

Journal Pre-proof

Table 1. A review for ionic liquid membrane including the type of materials, research objectives, computational details, application, and separation performance

Studies	Ionic liquid membrane	Study domains	Computation details	Application	Separation performance	Agreement with experimental results
(Abedini et al., 2017)	Ionic polyimides (i-PIs) i-PI+ionic liquid (IL) composite containing [C ₄ mim][Tf ₂ N]	Prediction of the gas molecules solubility and the adsorption for separation performance relative to the density, fractional free volume (FFV) and surface area of i-PIs and i-PI+[C ₄ mim][Tf ₂ N] computed using molecular dynamics and GCMC simulations.	-Simulation method: MD and GCMC - Software: GROningen Machine for Chemical Simulations (GROMACS) 5.0 - Forcefield: TraPPE	Gas separation for CO ₂ /CH ₄	During densification and relaxation of 55 monomers CO ₂ solubility is 4 g/L at 1.8g/cm ³ density and solubility increased to 14g/L at 1.58g/cm ³ density.	-
(Budhathoki et al., 2017)	1-n-butyl-3-methylimidazolium bis(trifluoromethyl sulfonyl)imide ([C ₄ mim] ⁺ [Tf ₂ N] ⁻ confined in carbon nanotubes and silica nanopores	Prediction of the self-diffusion coefficients of CO ₂ , CH ₄ , H ₂ and the gas mixtures by MD simulations and sorption isotherms of CO ₂ , CH ₄ , H ₂ , CO ₂ /CH ₄ and CO ₂ /H ₂ using MC simulations through graphite slit pores of 2nm and 5nm widths at 333K and pressures ranging from 1 bar to 200 bar (MC); to 100 bar (MD) with and without confined ionic liquid ([C ₄ mim] ⁺ [Tf ₂ N] ⁻) in the pores of carbon nanotubes and silica.	-Simulation method: MD and GEMC -Software: LAMMPS -Forcefield: TraPPE	Gas separation for CO ₂ /CH ₄	At pressure of 2 bar, the solubility of CO ₂ is 0.05 mole fraction for bulk IL, 0.1 for IL+2nm slit pore and 0.11 mole fraction for IL+5nm slit pore,	-
(Theng et al., 2017)	Polyvinylidene difluoride (PVDF) in [C ₂ bim] ⁺ and bromine anion ionic liquid	PVDF membrane with 50 wt%:50 wt% [C ₂ bim] ⁺ [Br] ⁻ :water and PVDF membrane with pure [C ₂ bim] ⁺ [Br] ⁻ are simulated to measure the P _e , RMSD, and RDF using molecular dynamics. Stability and interaction of PVDF+IL with penetrants were evaluated.	-Simulation method: MD -Software: GROMACS -Forcefield : OPLS	Wastewater separation	This articles revealed that PVDF has stronger interaction to [C ₂ bim] ⁺ cation (with shortest distance to PVDF after simulation) in comparison to water and bromine anion.	-
(Ying et al., 2018)	Laminated graphene oxide membrane with 1-butyl-3-methyl-imidazolium-tetrafluoroborate [BMIM][BF ₄] ionic liquid	The permeability and selectivity of CO ₂ through the CO ₂ -philic [BMIM][BF ₄] ionic liquid confined in nanochannels of laminated graphene oxide membrane are investigated.	-Simulation method: MD -Software: LAMMPS -Forcefield : OPLS-AA (GO structure) AMBER ([BMIM][BF ₄]) -Algorithm: SHAKE	Gas separation i.e. CO ₂ /H ₂ , CO ₂ /CH ₄ , CO ₂ /N ₂	Permeance of the facilitated CO ₂ transportation for the membrane: 68.5 GPU. Selectivities as follows: CO ₂ /H ₂ : 24 CO ₂ /CH ₄ : 234 CO ₂ /N ₂ : 382	-
(Zeng et al., 2018)	Room temperature ionic liquids (RTIL) confined in carbon nanotube (CNT) bundles RTIL used: [BMIM] ⁺ with [PF ₆] ⁻ , [SCN] ⁻ and [TF ₂ N] ⁻ anions.	Computation of adsorption and separation of CO ₂ from CO ₂ /N ₂ mixtures.[BMIM][PF ₆], [BMIM][SCN],	-Simulation method: MC -Software: RASPA 1.1	Gas separation i.e. CO ₂ /N ₂	Adsorption isotherm for CO ₂ using [BMIM][PF ₆] with carbon nanotubes has highest	-

Studies	Ionic liquid membrane	Study domains	Computation details	Application	Separation performance	Agreement with experimental results
		[BMIM][TF ₂ N] in CNT bundles was tested using GCMC simulations.	-Forcefield: UFF		loading of 1.1mol/kg at 100kPa.	
(Szala-Bilnik et al., 2019)	i-PI+IL composite membrane IL used: [BMIM] cation in combination with [PF ₆], [BF ₄] and [Tf ₂ N]	Investigated molecular level of ionic polyimides (i-PI) and i-PI+IL composite membrane gas adsorption and diffusion characteristics.	-Simulation method: MD and MC - Software: GROMACS - Forcefield: Liquid simulations-all atoms (AA)	CO ₂ capture	i-Polyimide with IL of [PF ₆] has the highest predicted CO ₂ solubility of 0.0275g/cm ³ at T _g of 355K.	-
(Tang et al., 2019)	Ionic liquid N-octylpyridinium bis(trifluoromethyl) sulfonyl imide [OPY][TF ₂ N] modified graphene oxide (IL-GO) incorporated into polyether block amide (PEBA)	Graphene oxide (GO) is modified with ionic liquid (IL) and then incorporated into PEBA membrane. GO and IL-GO is then studied for their water and butanol adsorption performance using molecular simulation. 0.4 wt%, 0.6 wt% and 1 wt% loading of IL- GO on PEBA membrane are investigated.	- Simulation method: MC - Software: Material Studio (MS) 7.0 - Forcefield: COMPASS II	Pervaporation of butanol aqueous solutions	1 wt% IL-GO-PEBA gives highest permeation flux of 460 g/(m ² h).	Pervaporation experiment results shows that IL-GO-PEBA membrane has better performance than pristine membrane with separation factor of 25.92 and permeation flux of 470.68g/(m ² .h).
(Song et al., 2019)	Ionic liquids (ILs) in poly(vinylidene fluoride) PVDF Ionic liquids used: [BMIM][PF ₆], [BMIM][TF ₂ N], and [BMIM][B(CN) ₄]	Investigated the interaction of ILs with PVDF, aggregation and separation efficiency using MD.	- Simulation method: MD - Software: GROMACS - Forcefield: All-atom (AA) Algorithm: LINCS	Gas separation for CO ₂ /N ₂	[BMIM][B(CN) ₄]/PVDF has largest solubility of CO ₂ and least degree of aggregation.	-
(Rahmani et al., 2020)	3D Graphene (3DGr) supported [EMIM][TF ₂ N]	Perform simulation to study separation performance of 3DGr supported IL.	- Simulation method: MD and MC - Software: LAMMPS Forcefield: AMBER	Gas separation for CO ₂ /CH ₄	The self-diffusion coefficient of 3DGr supported [EMIM][TF ₂ N] is 6 x 10 ¹¹ m ² /s	-
(Ishak et al., 2020)	[Chl][Ala]/IRMOF-1 composite membrane	Perform simulation to study the adsorption and stability of [Chl][Ala]/IRMOF-1 and its selective removal of H ₂ S/CO ₂ .	- Simulation method: MD - Software: GROMACS - Forcefield: OPLS - Algorithm: LINCS	Gas separation for H ₂ S/CO ₂	Results show preferred adsorption of H ₂ S with adsorption of A _{H₂S/CO₂} = 17.954 molL ⁻¹ bar ⁻¹ and adsorption selectivity of A _{H₂S/CO₂} = 43.159.	
(Cheng et al., 2021)	Ionic liquid in polyimide (PI) structure. PI structures: 6FDA-ODA, 6FDA-DPX and 6FDA-DAM Ionic liquid used: [EMIM] cation in combination with [PF ₆], [BF ₄] and [Tf ₂ N]	Author employed molecular design to improve the molecular sieve capability of imidazole ionic liquid in PI composite membrane.	- Simulation method: MD - Software LAMMPS	CO ₂ capture	6FDA-ODA (25% IL+PI) has the best performance with MSD of 10Å ² at 10ns, diffusion of 62 x 10 ⁻¹² m ² /s	-

Studies	Ionic liquid membrane	Study domains	Computation details	Application	Separation performance	Agreement with experimental results
	ILs/PI system: 25%[EMIM] [Tf ₂ N]/6FDA-ODA, 50%[EMIM] [Tf ₂ N]/6FDA-DPX, 75%[EMIM] [Tf ₂ N]/6FDA-DAM		- Forcefield: Union atom - Algorithm: SHAKE		when CO ₂ concentration is 27 wt%.	
(You et al., 2022)	[BMIM][Tf ₂ N]/polyimide (PI) composite membrane	Studied the effect of different IL concentration in the [BMIM][Tf ₂ N]/PI composite membrane in CO ₂ capture system.	- Simulation method: MD - Software: GROMACS - Forcefield: All-atom - Algorithm: LINCS	CO ₂ capture	The self-diffusion coefficient of [BMIM][Tf ₂ N] of 50 wt% in PI is $90 \times 10^{-11} \text{ m}^2 \text{ s}^{-1}$	-
(Yu et al., 2022)	[BMIM][Tf ₂ N]/ZIF-8	Simulation of IL encapsulated in ZIF-8 with detailed analysis of CO ₂ /CH ₄ diffusion including the adsorption capability and the study of gas diffusion routes.	- Simulation method: MD - Software: GROMACS - Forcefield: OPLS-AA - Algorithm: LINCS	Gas separation for CO ₂ /CH ₄	CO ₂ /CH ₄ adsorption ratio is doubled from 1.35 to 2.27 when IL is encapsulated to ZIF-8	Computed and experimental diffusion coefficient is in the same magnitude. Simulated diffusion coefficient: CO ₂ diffusing in [Bmim][Tf ₂ N]: $4.3 \times 10^{-11} \text{ m}^2 \text{ s}^{-1}$ Experimental diffusion coefficient: CO ₂ diffusing in [Emim][Tf ₂ N]: $4.3 \times 10^{-11} \text{ m}^2 \text{ s}^{-1}$ CO ₂ diffusing in [Omim][Tf ₂ N]: $1.7 \times 10^{-11} \text{ m}^2 \text{ s}^{-1}$

264 It was concluded that the cyclical relaxation between MD and GCMC can specifically increase the adsorption
Journal Pre-proof
265 of CO₂ (Abedini et al., 2017). The i-Pi polymer structure increasingly relaxed while alternating between MD and
266 GCMC, subsequently energy is lowered producing a more stable structure, accepting more CO₂. Addition of
267 [C₄mim][Tf₂N] ionic liquid to i-PI matrix improved the CO₂ adsorption and permeability, making a change on the
268 CO₂ and CH₄ favoured adsorption sites among ligand nitrogen and imidazolium nitrogen, but with negligible change
269 to relative adsorption of CO₂ and CH₄. The i-PI or IL can be functionalized to explore the possibility of increasing
270 the selectivity.

271 Owing to stronger gas-surface interactions in smaller pores, the decreased in pore width of the empty slit pores
272 increases the gas sorption in the sequence of CO₂ > CH₄ > H₂ due to stronger graphite interaction with CO₂ than
273 CH₄ and H₂ (Budhathoki et al., 2017). CO₂ interact with the pore walls of graphite with higher relative interaction
274 energy than CH₄ and H₂, while addition of [C₄mim][Tf₂N] further improved the adsorption of CO₂ in the ILM, with
275 3-4 times higher diffusion coefficient, higher adsorption capacity and solubility-selectivity of CO₂/CH₄ and CO₂/H₂
276 in 5nm graphite slit pore than 2nm graphite slit pore. This is due to IL density decrease with increasing graphite
277 pore width, providing more fractional free volume (FFV) creating more voids for CO₂ separation.

278 It was found that the ionic liquid can stabilize the PVDF structure by reducing the net repulsive force of the
279 model, the computed and measured potential energy and RMSD are lower especially when the ionic liquid weight
280 percentage is increased (Theng et al., 2017). RDF of [C₂bim]⁺ cation showed higher curve than [Br]⁻ signifying
281 that [C₂bim]⁺ has more interaction to PVDF than [Br]⁻.

282 [BMIM][BF₄] nanoconfined in laminated graphene oxide has higher resistance to high temperature, enhanced
283 durability and stability under high pressure with increasing CO₂ solubility and selectivity than other gases (Ying et
284 al., 2018). The increment of binding energy between CO₂ and GO-[BMIM][BF₄] promotes CO₂ solubility, due to
285 polarity of C=O bonds of CO₂ forming strong binding between CO₂ and [BF₄]⁻ anion, resulting in anion layer that
286 offers fast permeance and high selectivity. Increased thickness of GO/[BMIM][BF₄] membrane decreases the
287 permeances for each gas and increases CO₂ selectivity, with 1050nm found to be optimum thickness based on trade-
288 offs between the permeability and selectivity.

289 Introduction of ionic liquids into CNT channels has increased CO₂ adsorption while keeping the effect of N₂
290 adsorption at negligible level (Zeng et al., 2018). Strong interaction was observed between [BMIM][PF₆] confined
291 in CNTs and CO₂ gas molecules. However, CO₂ loading in ionic liquid was reduced under humid conditions, where
292 the modelled adsorption isotherm dropped more than half of the original performance in all ionic liquids.

293 Plasticization effect was observed on the i-PI with addition of ionic liquids leading to reduced T_g and calculated
Journal Pre-proof
294 theoretical surface area, but FFV remained the same. (Szala-Bilnik et al., 2019). $[PF_6^-]$ composite membrane has
295 the lowest T_g and $[Tf_2N^-]$ composite membrane has the highest T_g . T_g reduced with increased ionic liquid
296 concentrations above the threshold value of 30 mol%, facilitating CO_2 hopping rates from the void to void in the
297 composite membrane. At low ionic liquid concentration below the threshold value, blocking effect was observed
298 on the CO_2 transport. It was reported that their systems were about two orders of magnitude slower than the range
299 of various polymers disclosed in other studies.

300 It was found that $[OPY][Tf_2N^-]$ is hydrophobic with high affinity towards butanol (C_4H_9OH), confining
301 $[OPY][Tf_2N^-]$ to GO can prevent the pervaporation of IL, and effectively improve the membrane stability and
302 enhance the adsorption selectivity C_4H_9OH/H_2O by approximately 4 folds compared to pure GO (Tang et al., 2019).
303 IL-GO incorporated into PEBA membrane increased the permeation flux and separation factor of the ILM by 18.2%
304 and 31.5%.

305 CO_2 strongly interacts with ILs in which $[BMIM][B(CN_4)]/PVDF$ has the highest solubility compared to
306 $[BMIM][PF_6^-]/PVDF$ and $[BMIM][Tf_2N^-]/PVDF$ (Song et al., 2019). The hydrogen bond (HB) numbers decrease in
307 PVDF when IL concentration is increased improving the diffusion of CO_2 in PVDF chains, as the PVDF motion is
308 increased with lesser HB.

309 It was found that CO_2 diffusion coefficient increases with imidazole ionic liquid concentration (Cheng et al.,
310 2021). Increasing concentration of IL gradually decrease the coordination numbers of 6FDA-DPX (computed PI
311 structure). It indicates that the IL could have shielding effects that weakens the PI chains and ionic liquid interactions.
312 The interaction strength between the anions of IL and gas is in the sequence of $[PF_6^-] > [BF_4^-] > [Tf_2N^-]$. CO_2 are
313 more attracted to anhydride's partial nitrogen position (N1) in the sequence of 6FDA-ODA < 6FDA-DPX < 6FDA-
314 DAM PI structures.

315 It was observed that the incorporation of $[BMIM][Tf_2N^-]$ IL to PI initially decrease the self-diffusion coefficient
316 of CO_2 , the IL exhibited blocking effect as the IL are scattered in the composite membrane at low concentrations
317 reducing the FFV (You et al., 2022). As the IL concentration exceed 35 wt%, the IL started to form continuous
318 channels with increased FFV. HB number among PI chains decreased but HB number of PI with IL cation and anion
319 increased as IL concentration increase.

320 The liquid supported membrane is used extensively for the selective separation of harmful organic compounds
321 and CO_2 separation. Molecular simulation provides a mechanistic understanding of the adsorption, permeability,
322 diffusivity, and selectivity of the model. The relationship between the mechanistic study of ILM structure

323 compatibilities with the penetrants provides guidance for the design of the system. Molecular simulation model is
324 majorly based on MD and MC simulation method and the methods involved for molecular simulation is provided
325 in section 2 of this paper. MD simulation is a time-dependent evolution of the system and MC simulation involves
326 random sampling of the energy landscape to determine the probability with least value (Chen et al., 2020; Mehana
327 et al., 2021).. The model involved for simulation is provided in computation details in Table 1.

328 Most of the research group computed ILM for sour gas separation especially CO₂ from CH₄ and N₂ (Gonzalez-
329 Miquel et al., 2011; Budhathoki et al., 2017; Mohammadi et al., 2018; Szala-Bilnik et al., 2019; Cheng et al., 2021).
330 Limited study of computed hybrid membranes are found in other applications such as wastewater treatment (Theng
331 et al., 2017) and pervaporation (Tang et al., 2019). Hybrid membrane is widely applied in many sectors including
332 wastewater treatment, water purification, biogas purification, and etc. Hybrid membrane in CO₂ separation is an
333 emerging sector and most computational research revolves around CO₂ separation; currently, there is scarce
334 computational research for liquid separation and mainly limited to water treatment (Wei et al., 2020; Xu and Jiang,
335 2020).

336 Imidazolium based cation was mostly applied during molecular simulation of ILM mainly due to its negligible
337 vapor pressure, good extracting ability and thermal stability (Singh et al., 2018; Subasree and Selvi, 2020). [PF₆]⁻
338 and [Tf₂N]⁻ anions have been computed in the ILMs more often than other available anions especially for CO₂ gas
339 removals (Zeng et al., 2018; Szala-Bilnik et al., 2019; Cheng et al., 2021). This is due to its adsorption ability and
340 lower T_g .

341 None of the work has reported on the molecular computation of recycling of the ionic liquid in the membrane
342 when it is saturated and the long-term stability of the ILM. Saturation of contaminants in membrane material is a
343 factor for fouling. Membrane regeneration is one of the solutions for this issue (Deqian, 1987). Regeneration
344 techniques for contaminants saturated membrane includes physical, chemical, and physio-chemical methods
345 (Deqian, 1987; Ebrahim, 1994). However, the regeneration is a process, which is difficult to be carried out using
346 molecular simulations software thus far. It is challenging to simulate a chemical reaction equilibrium molecularly
347 (Smith and Qi, 2018). Additionally, the function is challenging and computationally expensive because MD-based
348 future predictions are only about the next 2-3 s of the processes (Mollahosseini and Abdelrasoul, 2021). Despite
349 algorithm advancements, characterizing various types of motion in macromolecular systems that involve extremely
350 broad range of time scales, which is typically applicable to glassy state membrane that requires time scale from tens
351 of femtoseconds (covalent bond vibrations) to years (long-term stability), is not realizable. In this regard, MD is an

Theodorou, 2019).

The common forcefield used for simulation of ILM model includes AMBER, COMPASS, and OPLS All-Atom (AA). AMBER forcefield covers all parameters to facilitate simulation of organic molecules like ionic liquids (Cornell et al., 1995), COMPASS forcefield covers broad range of organic polymers and inorganic with organic hybrid membrane (Asche et al., 2017); while OPLS All-Atom can reproduce organic liquids' condensed phase properties accurately (Murzyn et al., 2013).

Key accomplishments in addition of IL to MMM may improve the permeability, the selectivity, or both, synergising with filler. They combine the advantage of easy operation of membrane and high solubility liquid stripping process. Molecular simulations aided in screening of IL in membrane (Gonzalez-Miquel et al., 2011; Song et al., 2019) without needing to perform various costly experiments at the preliminary stage.

3.2 Mixed Matrix Membrane

Molecular simulation enables the study of interaction of the molecules in MMM, important and crucial data such as permselectivity, FFV, density analysis, XRD are some of the parameters that could be simulated and analysed prior to experimental analysis. Molecular studies of MMMs, their application and separation performance are summarized in Table 2. Figure 3 shows the molecular dynamics simulation for MMM and the molecular view of the system.

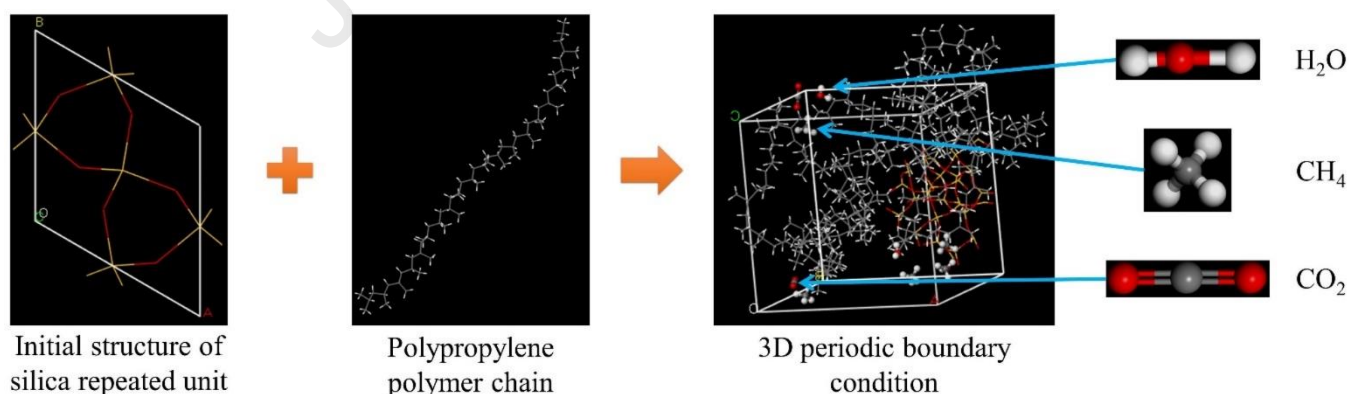


Fig. 3 The configuration of constructed MMM of polypropylene polymer (white) and SiO₂ (red-orange). Its interactions with feed and permeate gas (H₂O, CH₄ and CO₂) are shown.

Table 2 A review of mixed matrix membrane including the type of materials, research objectives, computational details, application, and separation performance

Studies	Mixed matrix membrane	Study Domain	Computation Details	Application	Separation Performance	Agreement with experimental results
(Keskin, 2010)	Zn(bdc)(ted) _{0.5} (zn = zinc; bdc = 1,4-benzenedicarboxylic acid; ted = triethylenediamine)	Self-diffusivities and adsorption isotherms with different composition of Zn(bdc)(ted) _{0.5} , computed using MD simulations at room temperature	- Simulation method: MD and MC - Forcefield: Universal	Gas separation for CH ₄ /H ₂	At fugacity of 10bar, Zn(bdc)(ted) _{0.5} has adsorptive selectivity of 50 for CH ₄ /H ₂ .	-
(Golzar et al., 2014)	Nanosized silica particles filled poly(oxy-1,4-phenylenesulf-onyl-1,4-phenyleneoxy-1,4-phenyleneisopropylidene1,4-phenylene) (PSF) membranes	Prediction of the diffusivity and solubility of gases including nitrogen, oxygen, carbon dioxide and methane through the MMM using MD. Studied the transport behaviours of gases in the PSF nanocomposite with different concentration of the nanosized silica particles membranes.	- Simulation method: MD and MC - Software: Material studio - Forcefield: COMPASS - Algorithm: Metropolis	Gas separation for CO ₂ /CH ₄ , CO ₂ /N ₂ , CO ₂ , O ₂	At 20% silica and 80% polysulfone, the predicted diffusivity of O ₂ , N ₂ , CO ₂ and CH ₄ are 16.05, 6.41, 5.21 and 1.89 (x 10 ⁻⁸ cm ² /s).	Simulated diffusivity and experimental diffusivity of O ₂ , N ₂ , CO ₂ , CH ₄ have difference of 20-30%.
(Wang et al., 2016a)	Amorphous poly(ether imide) (PEI) polymer with boron nitride nanotubes (BNNT) BNNTs of the zigzag types, nanotubes of (3,0), (7,0) and (12,0) nanotubes with diameters of 9.5Å, 5.6Å, 2.5Å. The three polymer composites are named PC3, PC7 and PC12.	Prediction of the possibility of utilize a new type of polymer composites namely the amorphous poly(ether imide) (PEI) and boron nitride nanotubes (BNNTs). The diffusivities, solubilities and FFV in the PEI-BNNTs composites were computed using MD.	- Simulation method: MD - Forcefield: Universal	Gas separation for CO ₂ /CH ₄	PC12 has the highest computed solubility of 105.55cm ³ /atm of CO ₂ .	PEI simulated solubility and measured solubility of CO ₂ has a difference of 35%.
(Dehghani et al., 2017)	Poly (amide-6-b-ethylene oxide) (PEBA 1657)/ Faujasite (FAU)	Poly (amide-6-b-ethylene oxide) (PEBA 1657)/Faujasite (FAU) mixed matrix membrane is simulated to study the structural and transport properties.	- Simulation method: MC - Software: Materials Studio - Forcefield: COMPASS - Algorithm Metropolis	Gas separation for CO ₂ /N ₂	PEBA 1657/Faujasite has a T _g of 204.1K. The CO ₂ diffusivity is 0.0517 and CO ₂ permeability is 89.23 Barrer with FAU composite of 20% at 298K.	-
(Hwang et al., 2018)	ZIF-8 metal organic framework dispersed in 6FDA-DAM polymer	Applied molecular modelling to microscopically study on the MOF/polymer. A record on the change of CO ₂ concentration in the ZIF-8/6FDA-DAM membrane is unfolded through microimaging by IR microscopy.	- Simulation method: MD and MC - Forcefield: AMBER	Gas removal for CO ₂	Atomic simulations revealed the presence of the microvoids of 9Å at the MOF/polymer interface and accumulation of CO ₂ in these microvoids.	-
(Tan et al., 2018)	- Zeolitic imidazole framework-8 (ZIF-8)-Polyimide (PI) - Alumina-PI	In depth study of 3-(aminopropyl)triethoxysilane (APTES) for promoting the synthesis of polyimide (PI)/zeolitic imidazole framework-8 (ZIF-8) and alumina/PI MMMs experimentally and verified through molecular simulation	- Simulation method: MD - Forcefield: Material Studio	Gas separation i.e. CO ₂ /N ₂	PI/ZIF composite membrane with 3 layers of polyimide base gives Permeance: 93.47 GPU CO ₂ /N ₂ selectivity: 7.50.	-

(Kong and Liu, 2019)	Porous organic cage (POC)/ polymer of intrinsic microporosity (PIM-1) Discrete CC3 cages/PIM-1 -> micromixed MMM CC3 crystal/PIM-1 -> macromixed MMM	Construction of macromixed and micromixed MMM of a CC3 and PIM-1 using MD to assess permeability and steady state adsorption amount of CO ₂ and N ₂ at pressure from 1-13 bar, selectivity, diffusivity, density, void size distribution and free volume.	- Simulation method: MD - Software: GROMACS - Forcefield: OPLS-AA	Gas separation for CO ₂ /N ₂	Macromixed MMM (MMM-83) has permeability of 44000barrer and selectivity of 10.4, highest performance among other membrane composite.	
(Liu et al., 2019b)	Pebax-1657-based mixed matrix membrane doped with MoS ₂ nanosheets	Applied molecular simulation on Pebax-1657 based membrane doped with MoS ₂ nanosheets to study the CO ₂ solubility and CO ₂ /N ₂ solubility selectivity. Characterization is done on the fabricated MMM as well.	- Simulation method: MD - Software: Material Studio - Forcefield: PCFF	Gas separation i.e. CO ₂ /N ₂	Pebax membrane doped with 4.76 wt% MoS ₂ nanosheets had the best performance, with CO ₂ permeability of 67.05 barrer and CO ₂ /N ₂ selectivity of 90.61.	Highly correlated with experimental results.
(Monsalve-Bravo et al., 2020)	Polyimide based MMM with MFY-type zeolite Polyimide based MMM with carbon molecular sieve (CMS)	Employed equilibrium molecular dynamics to assess the permeation of gas through MMM with interfacial defects.	- Simulation method: MD and MC - Software: LAMMPS - Forcefield: PCFF - Algorithm: Force-Biased (FBA)	Gas separation i.e. CO ₂ /CH ₄	PI/CMS based MMM has Permeability: 18 Barrer CO ₂ /CH ₄ selectivity: 70	Simulated and experimental permeability and selectivity has percent error of 5%.
(Riasat Harami et al., 2019)	Zeolite 4A embedded into polydimethylsiloxane (PDMS)	Elaboration of the physical movements of molecules and understanding the structural properties and identifying the solubility coefficients of CO ₂ , CH ₄ , C ₃ H ₈ and H ₂ gaseous molecules in PDMS/Zeolite 4A of different loadings.	- Simulation method: MD and MC - Software: Material Studio - Forcefield: COMPASS	Gas separation	CO ₂ solubility coefficient at 298K with 10 wt% zeolite 4A in PDMS is $33.10 \times 10^{-4} \text{ cm}^3(\text{STP})/\text{cm}^3(\text{polymer})\text{cmHg}$	Solubility of H ₂ at 318K in simulation and experimental results has percent error of <5%.
(Amirkhani et al., 2020)	Poly(ether-b-amide) (PEBA) filled by different amounts of nano ZnO (0, 0.1, 0.3, 0.5 0.75 and 1 wt %)	Fabricated ZnO filled PEBA MMMs for characterization with permeability and <i>T_g</i> investigated experimentally. Prediction on the structural properties and gas transport performance is simulated.	- Simulation method: MD and MC - Software: Materials Studio - Forcefield: COMPASS - Algorithm: Verlet	Gas separation i.e. CO ₂ /CH ₄ , CO ₂ /N ₂	At 0.5 wt% loading of ZnO, the MMM, CO ₂ Solubility: $3.97 \times 10^{-3} \text{ cm}^3(\text{STP})/\text{cm}^3(\text{polymer})\text{cmHg}$ CO ₂ Diffusivity: $33.3 \times 10^{-7}(\text{cm}^2\text{s}^{-1})$ Permeability: 132.29 Barrer.	CO ₂ permeability and CO ₂ /CH ₄ selectivity were reduced compared to single gas experiments.
(Lock and Yiin, 2020)	α -Quartz/PSF α -Cristobalite/PSF α -Tridymite/PSF (PSF with 15, 20, 25, 30, 35 wt% amount of silica polymorphs)	Pioneered in simulation of incorporation of nanosized SiO ₂ in the form of varying polymorph configurations (α -Quartz, α -Cristobalite, α -Tridymite) into Polysulfone (PSF) to investigate its feasibility to improve gas separation.	- Simulation method: MD - Software: Materials Studio - Forcefield: COMPASS	Gas separation i.e. CO ₂ /CH ₄	PSF with 25 wt% of α -Cristobalite at 25°C has CO ₂ Solubility: $5.31 \text{ cm}^3(\text{STP})/\text{cm}^3$ [STP]cmHg CO ₂ Diffusivity: $5.72 \times 10^{-8} \text{ cm}^2/\text{s}$ CO ₂ Permeability: 39.98 barrer	-

(Riasat Harami et al., 2020)	Polycarbonate (PC)/p-nitroaniline(pNA)/zeolite 4A	Molecular simulation to determine the diffusivity and solubility coefficients of gas molecules within the MMM.	- Simulation method: MD and MC - Software: Materials Studio Forcefield: COMPASS	Gas separation	Neat PC CO ₂ Diffusivity: 4.01×10^{-7} cm ² /s CO ₂ Permeability: 7.21 Barrer PC/5% pNA/30% 4A CO ₂ Diffusivity: 1.94×10^{-7} cm ² /s CO ₂ Permeability: 4.05 Barrer	-
(Wei et al., 2020)	Polyacrylate (PAR) / Zeolitic-Imidazolate Framework (ZIF-8 and ZIF-93)	Prediction of the performance on desalination of water of PAR/ZIF and the swelling degree of the MMM.	- Simulation method: MD - Software: GROMACS - Forcefield: OPLS-AA	Water desalination	All MMMs rejects 100% of sodium and chloride ions.	-
(Zhao and Jiang, 2020)	Porous organic cage (POC) incorporated into polymer of intrinsic microporosity (PIM-1): MMM1 (1 cage/13 PIM-1 chains) MMM2 (1 cage/20 PIM-1 chains) MMM3 (1 cage/28 PIM-1 chains)	Studied the MMMs formed by POC(PB-1A)/PIM-1 on their degree of swelling, salt rejection and water permeability using molecular simulation	- Simulation method: MD - Software: GROMACS - Forcefield: OPLS-AA - Algorithm: Leap-frog	Water desalination	MMM1 has the highest permeability of 10^{-5} kgm/m ² hbar and 99% salt rejection. MMM2 and MMM3 has 100% salt rejection but permeability of $<10^{-5}$, $>10^{-6}$.	-
(Asif et al., 2021)	Silica/polysulfone for separation of gas with varying concentrations (i.e., 30% CO ₂ /CH ₄ , 50% CO ₂ /CH ₄ , and 70% CO ₂ /CH ₄) and silica content (i.e., 15–30 wt%)	Performed molecular simulation to predict the solubility, diffusivity and selectivity of CO ₂ /CH ₄ through the silica/polysulfone MMM with different gas concentrations and silica content. The respective separation performances are investigated.	Simulation method: MD and MC Software: Materials Studio Forcefield: COMPASS	Gas separation for CO ₂ /CH ₄	15 wt% of silica in PSF has lowest CO ₂ solubility of 2.0 cm ³ (STP)/cm ³ atm but highest solubility selectivity of CO ₂ /CH ₄ of 30. The solubility and selectivity provided is at 30% CO ₂ /CH ₄ .	Simulated and experimental density has less percent error of <5%.
(Salahshoori et al., 2021b)	Polysulfone-polyethylene glycol-silica (PSF-PEG-Silica)	Studied the effect of silica loading, temperature, and pressure on the transport performance for CO ₂ , CH ₄ and N ₂ gases.	Simulation method: MC and MD Software: Material Studio Forcefield: COMPASS	Gas separation for CO ₂ /CH ₄ and CO ₂ /N ₂	20 wt% of silica incorporated to PSF-PEG MMM at 25°C and 10 bar gives CO ₂ permeability of 14.76 Barrer CO ₂ /CH ₄ selectivity of: 25.44	

376 It is observed that there is high adsorption selectivity of CH₄ using Zn(bdc)(ted)_{0.5} and high permeance for H₂
377 (Keskin, 2010). H₂ molecules are relatively small to the pore size resulting in the high permeance and faster diffusion
378 through the MMM resulting in higher H₂/CH₄ selectivity. The adsorption selectivity using Zn(bdc)(ted)_{0.5} is claimed
379 to be notably higher than different MOFs, IRMOF-1, IRMOF-8, IRMOF-10, and CuBTC. The calculations are
380 performed with the assumption of ideal condition of the membrane.

381 Incorporation of silica to PSF matrix reduced and disrupted the efficient chain packing of PSF, producing
382 microvoids in the matrix of the PSF membrane (Golzar et al., 2014). This increases the FFV and average cavity
383 size. Thus, the separation performance and transport properties of the PSF/silica MMM is more superior than pure
384 polysulfone membrane.

385 The BNNT nanotubes in the polymer created larger fluctuation in free volume distribution as demonstrated in
386 the cavity size distribution of the composite membrane improving the solubilities and self-diffusivities of CO₂ in
387 polymer-BNNT, facilitating gas permeabilities and separation properties (Wang et al., 2016a). This is evident via
388 increased concentration of gas molecules within the membrane materials as reported by C. Wang et. al.

389 With the addition of 20 wt% of FAU nanomaterials, the CO₂ permeability increases with a decrease of T_g as
390 compared to pure PEBA 1657 (Dehghani et al., 2017). It was predicted that both the transport and structural
391 properties are enhanced due to the more pathways that facilitates CO₂ transport through the membranes. Presence
392 of pores in FAU increases the pathways, increasing its concentration would improve the permeability of penetrant
393 molecules.

394 The MOF/polymer interface is observed to have microvoids formation and is more pronounced at high pressure
395 (Hwang et al., 2018). The weak interactions of -OH and -NH at ZIF-8 surface and -CF₃, -CH₃ and -CO at 6FDA-
396 DAM resulted in well-defined microvoids delimited by anchoring points of the molecules' interaction. The CO₂
397 molecules accumulation are preferred at these microvoids indicating that there might be a layer at the interface of
398 MOF serving as the initial step of mechanism with high CO₂ affinity. It serves an indication of filler-polymer
399 compatibility. From the IR time resolved images, it is found that CO₂ molecules transport through the filler, which
400 may imply the CO₂ mass transport through the "highway" especially at high pressure. Similar transport patterns
401 were predicted in molecular dynamics.

402 It is found that APTES treated alumina can improve adhesion between alumina-PI during synthesis allowing
403 formation of up to 5 layers of defect-free PI dip-coated alumina-supported PI membrane with improved
404 compatibility (Tan et al., 2018). Molecular simulation demonstrated lower binding energy (-16.00 kcal/mol) for

405 model containing APTES than model without APTES (26.96 kcal/mol) indicating stable membrane system with the
Journal Pre-proof
406 presence of APTES.

407 There is no profound improvement of CO₂ permeability when discrete CC3 molecules are dispersed in the
408 PIM-1 membrane matrix in micromixed MMMs; while there is notable enhancement of gas permeability without
409 selectivity trade-off in macromixed MMMs (Kong and Liu, 2019). The micromixed MMM is constructed by adding
410 CC3 cages, while macromixed MMM is constructed by adding CC3 crystal. The gas permeation performance for
411 both type of MMMs is different because macromixed CC3 crystal disturb the packing of PIM-1 chains creating
412 reasonably large pores in the interface, promoting gas permeation; while PIM-1 can pack tightly around the
413 micromixed CC3 cage resulting in no notable change in void size distribution with no performance improvement.

414 It is observed that the MMM has strong affinity towards CO₂ due to added MoS₂ in the MMM which
415 contributes to high CO₂/N₂ selectivity (Liu et al., 2019b). The adsorption of CO₂ molecules increased with
416 increasing pressure indicating that the simulated results agree with rubbery polymer matrix properties, in which the
417 sorption behaviour is usually related to Henry's Law.

418 For both of the polyimide based MMM with MFY type zeolites and CMS, it is observed that there is polymer
419 rigidification with reduced permeability at the interfacial region of the polymer-adsorbent interface in non-ideal
420 simulations (Monsalve-Bravo et al., 2020). Macroscale simulations reveal that if the filler particle size is optimum,
421 it can maximize the permeability of gas in non-ideal MMMs. The CO₂/CH₄ permselectivity is influenced by the
422 finite uniform and non-uniform particle size distribution's interfacial resistance. Particle size distribution (PSD)
423 effect on gas permeability performance is investigated in ideal and non-ideal conditions of the MMMs. The non-
424 uniform PSD in ideal condition has negligible effect to the permeability while in ideal condition it has more notable
425 effect to the permeability. This work is one of the first fundamental approach in studying both ideal and non-ideal
426 MMMs in simulation.

427 The gas solubility coefficients are found to be in decreasing order of C₃H₈ > CO₂ > H₂ > CH₄ through the MMM
428 (Riasat Harami et al., 2019). The article demonstrated that higher zeolite content increases the T_g and decreases the
429 gas solubility. This could be due to the non-sorbent zeolite materials substituted fraction of polymer chains, which
430 adsorb gaseous molecules less effectively, as explained by H. Riasat Harami et. al. The reduction in solubility is in
431 agreement with other experimental research (Adams et al., 2011; Tahir et al., 2018). With further zeolite loading,
432 the solubility reduction effect decreases due to more channels and pores from the increased loading amount of
433 zeolite 4A nanoparticles (Riasat Harami et al., 2019). The MMM is capable to adsorb more gas molecules in lower
434 temperature than higher temperature.

435 It was revealed that PEBA membrane loaded with 0.5 wt% ZnO results in increased permeability for CO₂
436 compared to the pristine PEBA membrane as the FFV is found to increase (Amirkhani et al., 2020). Higher CO₂
437 permeability is acquired when the feed pressure and temperature is increased while CH₄ and N₂ has negligible
438 changes on the transport performance. The plasticization effect of the MMM stimulates gas transport.

439 The increment weight percentage of silica polymorphs, as the inorganic filler, increases the free volume and
440 T_g , which translates to the enhancement of the gas solubility, diffusivity and permeability of CO₂ and CH₄ but
441 compromised on its CO₂/CH₄ selectivity (Lock and Yiin, 2020). The increase in free volume is due to the inorganic
442 filler disrupting the polymer chain packing creating bigger void spaces. The addition of silica polymorphs has
443 reduced the mobility of the polymer chain causing increment of the T_g , in consistent with experimental findings
444 (Ahmad et al., 2015; Najafi et al., 2018; Vatanpour et al., 2022). It is predicted that the most optimum MMM
445 according to gas permeability enhancement is addition of 25 wt% of α -Cristobalite, a polymorph configuration of
446 SiO₂, to polysulfone matrix. This work has pioneered in molecular simulation study of SiO₂ polymorphs for
447 enhancement of gas separation.

448 When zeolite and pNA is incorporated into PC, deterioration of permeability is observed which can be
449 associated with the gas kinetic diameter where CH₄ has the most significant reduction while O₂ and H₂ has the least
450 reduction (Riasat Harami et al., 2020).

451 It is found that in different PAR/ZIF MMMs, PAR of bulk region demonstrated same swelling degree and void
452 size distribution (from $<5\text{\AA}$ enlarged up to 13\AA) (Wei et al., 2020). This implies that the presence of ZIF mostly
453 does not affect the microstructure of PAR. Due to hydrophobic characteristic of ZIF-8, during swelling, the
454 PAR/ZIF-8 interface stays intact, exhibiting comparable interaction with PAR and water. ZIF-93 is hydrophilic with
455 considerably stronger interaction with water than the polymer matrix, PAR. Increasing ZIF content in PAR/ZIF-8
456 membrane decreases the permeability of water but for PAR/ZIF-93 MMMs the water permeability remains the same.
457 All the MMMs can reject salt permeation. Hydrated diameter of Na⁺ (7.16\AA) and Cl⁻ (3.7\AA) ions are bigger than
458 ZIF-8 (3.4\AA) and ZIF-93 (3.7\AA), enabling MMMs to retain the salt molecules.

459 3 MMMs are constructed with different POC/PIM-1 ratios for water desalination with MMM1, MMM2, and
460 MMM3 having 1 POC/13 PIM-1 chains, 1 POC/20 PIM-1 chains, and 1 POC/28 PIM-1 chains, respectively (Zhao
461 and Jiang, 2020). The swelling degrees are 69.3% in MMM1, 64.9% in MMM2 and 56.6% in MMM3 higher than
462 the swelling degrees in pristine PIM-1 membrane. This is because embedding porous PB-1A cage to PIM-1
463 increases the free volume of MMM. MMM1 rejects approximately 99% of salt, while MMM2 and MMM3 rejects
464 100% of salt. MMM1 is the thinnest, most porous and allows ions to permeate, while MMM2 and MMM3 the PIM-

20–30% separation performance from pure PIM-1 as reported by Z. Zhao and J. Jiang.

As the gas concentrations increase, the gas permeation for gas mixture also increases in the following order $70\% \text{ CO}_2/\text{CH}_4 > 50\% \text{ CO}_2/\text{CH}_4 > 30\% \text{ CO}_2/\text{CH}_4$ (Asif et al., 2021). As the silica content incorporated in polysulfone increases, the transport properties including diffusivity, solubility, and permeability of the penetrant molecules are steadily increasing until 25 wt.% of silica contents, followed by a decrease of the transport properties with 30 wt.% of silica contents. The enhancement of the diffusion of the binary gases is because of more void space when silica weight percentage is increased.

The incorporation of silica into PSF-PEG MMM improved the permeability and selectivity (Salahshoori et al., 2021b). The silica nanoparticles prevent softening effect of CO_2 on the polymeric membranes by reducing the mobility of the polymeric chains improving membrane rigidity, and the strong interactions of silica with CO_2 molecules improves the selectivity of CO_2 (Salahshoori et al., 2021b). The increase in permeability could be due to the selective surface area when silica nanoparticles are uniformly distributed in the polymer matrix (Salahshoori et al., 2021a). It could also be due to the interaction of the polymer chain with silica via hydrogen bonding, increasing the solubility of polar gases, in this case CO_2 (Golzar et al., 2017a; Setiawan and Chiang, 2019).

Computation of MMM mainly focuses on CO_2 separation from CH_4 followed by CO_2 removal from N_2 and O_2 (Kong and Liu, 2019; Liu et al., 2019b; Riasat Harami et al., 2019; Lock and Yiin, 2020; Monsalve-Bravo et al., 2020). Limited works have reported on computation of MMM for water treatment (Wei et al., 2020; Zhao and Jiang, 2020).

Metal organic frameworks particularly ZIF-8 is mostly used for dispersion into a polymer matrix during molecular simulation (Hwang et al., 2018; Tan et al., 2018; Wei et al., 2020) followed by silica (Golzar et al., 2014; Asif et al., 2021).

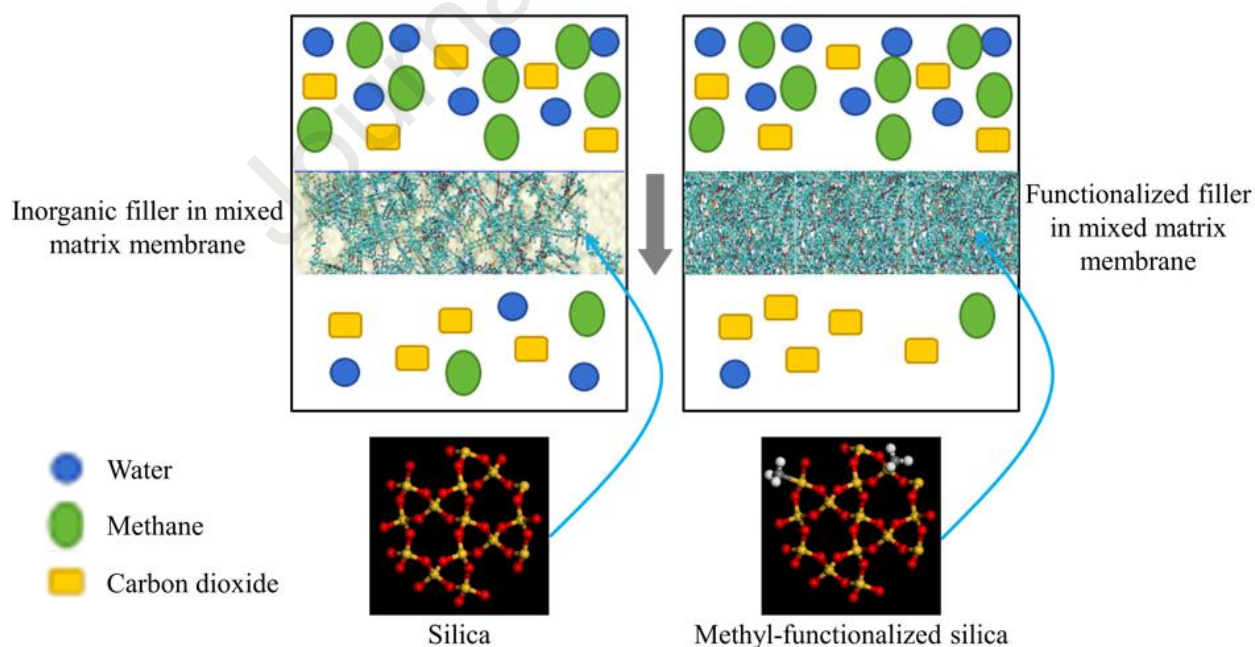
Majority of the research work focused on the accuracy of computed separation performance and properties of the inorganic membrane incorporated into polymeric membrane but however overlooked the transport performance of the membrane as the membrane physically aged and the possibility of plasticization by the inorganic filler. The solubility, selectivity, permeability, and durability of the membrane in long term application lacks study due the limitation of computational method not being able to simulate the physical aging because of the time span and physical wear and tear that could not be naturally occurring in simulation.

MMM with different inorganic fillers that are studied using molecular simulation studies are emerging, including metal oxide-based MMMs, particularly SiO_2 , MOF based MMM, zeolite based MMM, and CNT based

495 MMM. Metal oxides are most widely accepted inorganic fillers for improvement of membrane by their different
496 pore size, increasing chain mobility of membrane, low cost, good availability and so on (Zhu et al., 2021). MOF
497 have ultra-high surface area, with higher packing capacity, low density, etc (Qian et al., 2020). Zeolite has gained
498 much attention in gas separation in recent years due to its insolubility in water, microporosity, and wide range of
499 structure with molecule sized dimension (Krishna and van Baten, 2010). CNT can be categorized into single walled
500 CNT (SWCNT) and multi walled CNT (MWCNT) and the properties are very attractive due to their high aspect
501 ratio (length to diameter), high thermal conductivity, flexible, etc (Wang et al., 2020).

502 From the molecular simulation studies, higher amount of filler tends to agglomerate and form clusters in the
503 polymer membrane (Kim et al., 2007). Appropriate amount of filler in the polymer chain matrix is found to disrupt
504 the polymeric chain of the membrane, producing more voids and subsequently more FFV that facilitates molecules
505 permeation (Kim et al., 2007; Golzar et al., 2014; Lock and Yiin, 2020). With molecular simulation tools, the
506 intrinsic properties of MMM such as the molecular sieving ability, dispersion ability, surface area and transport
507 performance can be decoded (Riasat Harami et al., 2019).

509 Hybrid membrane functionalization is one of the efficient techniques to further enhance properties of the
 510 membrane. Its application to hybrid membranes in many fields has progressed rapidly in recent years especially in
 511 carbon capture and storage. The functionalities can be thoughtfully tailored to reduce membrane swelling issue,
 512 increasing both permeability and selectivity, and increase the strength of the membrane for large scale application.
 513 From Table 3, applications of molecular simulation for functionalized polymer in fermentation, gas separation,
 514 biomedical application such as purification of medicine from natural source are enumerated. Surface modification
 515 processes via different methods have been assessed and developed for the membrane with enhanced properties.
 516 Mostly, researchers can study on the non-bonded forces, the van der Waals force, interfacial energy, RDF, solubility
 517 coefficient and intrinsic characteristics of the modified membrane using molecular simulations.
 518 Figure 4 illustrates the performance of functionalized hybrid membrane which improves the MMM's
 519 hydrophobicity, compared to a normal hybrid membrane. The left hybrid membrane in Figure 4 illustrates
 520 membrane swelling when solvent molecules permeate into the membrane matrix, occupying the voids of the
 521 membrane and subsequently dilate the membrane; while the right hybrid membrane in Figure 4 illustrates the
 522 functionalized hybrid membrane without swelling.



523

524 **Fig. 4** A graphical illustration of functionalization of hybrid membrane in improving separation performance in
 525 both selectivity and permeability with improved membrane characteristic of its hydrophobicity (reduce membrane
 526 swelling issue) with the functionalization of the silica with hydrophobic functional group (Lee et al., 2022). Figure
 527 adapted from (Liu et al., 2019a).

Table 3 A review of functionalized hybrid membrane including the type of materials, research objectives, computational details, application, and separation performance

Reference	Functionalized Hybrid Membrane	Study Domain	Computation Details	Application	Separation Performance	Agreement with experimental results
(Kim et al., 2007)	Single walled carbon nanotubes (SWNT) functionalized with octadecylammonium (ODA) and polysulfone (PSF) as the polymer matrix	Fabrication of SWNTs functionalized ODA dispersed in polysulfone polymer matrix nanocomposite membranes. Gas adsorption and permeability performance were investigated using the MMM prepared.	Simulation method: MC	Gas separation for CO ₂ /CH ₄	10 wt% SWNT/PSF has: CO ₂ permeability of 5.19 Barrer CO ₂ diffusivity of $6.48 \pm 0.51 \times 10^{-8}$ cm ² /s	-
(Yani and Lamm, 2009)	Octahydro silesquioxane (OHS) or octaaminophenyl silsesquioxane (OAPS) functionalized polyhedral oligomeric silesquioxanes (POSS) with polyimide (PI) as polymer matrix	Applied MD for molecular understanding of PI and POSS MMM behaviour. The effect of functional groups OHS and OAPS on PI are examined. The Glass transition temperature (T_g), radial distribution function and PI chains mobility with POSS molecules in the functionalized MMM are determined.	- Simulation method: MD - Software: LAMMPS - Forcefield: Hybrid-COMPASS	Gas separation	Mean Square Displacement of 10.45 wt% OHS-POSS/PI is 63Å, highest as compared to other functionalized membrane loaded at different weight percent.	-
(Kasahara et al., 2016)	Amino acid ionic liquids (AAILs) with polytetrafluoroethylene (PTFE).	Prediction of the AAILs/PTFE membrane's physical properties including the density, viscosity, FFV and transport properties such as N ₂ /CO ₂ absorption capacities using molecular dynamics.	- Simulation method: MD - Software: MS + GROMACS - Forcefield: AMBER - Algorithm: LINC	Gas separation for CO ₂ /N ₂	[aN ₁₁₁ [Gly]-based FTM at 5kPa CO ₂ partial pressure has: CO ₂ permeability of 3000 Barrer CO ₂ /N ₂ selectivity of 110	-
(Park et al., 2016)	Polar groups -OH or -NH ₂ functionalized multi walled carbon nanotubes (MWCNTs) and co-polyimide (P84)	The macroscopic CNT dispersion through P84 matrix is examined for its transport behaviour using MD and macroscopic CNT dispersion in P84 matrix using mesoscale simulations	- Simulation method: MD and mesoscale simulation - Software: Materials Studio - Forcefield: COMPASS forcefield	Water treatment	MWCNT of hydroxyl groups functionalized CNT has solubility parameter of 23.2 ± 1.3 (J/cm ³) ^{1/2} MWCNT of amine groups functionalized CNT (CNT-NH ₂) has solubility parameter of 24.2 ± 1.0 (J/cm ³) ^{1/2}	Both simulated and experimental results show non-functionalized MWCNT and P84 are not compatible.
(Golzar et al., 2017b)	- 0.5-3.0 wt% Pristine single-walled carbon nanotubes (p-SWCNT) embedded into PIM-1 - 0.5-3.0 wt% Pristine multi-walled carbon nanotubes (p-MWCNT) embedded into PIM-1 - Polyethylene glycol (PEG) functionalized SWCNT (f-SWCNT) embedded into PIM-1	Prediction of the transport properties of gas mixtures including CO ₂ , CH ₄ , N ₂ and O ₂ into the pristine PIM-1 membrane and MMM based on PIM-1 using molecular simulations.	- Simulation method: MD and GCMC - Software: Materials Studio - Forcefield: PCFF	Gas separation CO ₂ /CH ₄ , CO ₂ /N ₂ , CO ₂ /O ₂	PIM/f-SWCNT(2%) is the MMM that have highest diffusivity of $24.76 \pm 4.78 \times 10^7$ cm ² /s and high solubility of $789.54 \pm 89.43 \times 10^3$ cm ³ (STP)/cm ³ (PIM/f-SWCNT)cmHg	The simulated density and the available experimental density of the membranes have percent error of <5%.

	- Polyethylene glycol (PEG) functionalized MWCNT (<i>f</i> -MWCNT) embedded into PIM-1		- Algorithm: Verlet			
(Pazirofteh et al., 2017)	Polyethylene (PEG) functionalized Polyhedral oligomeric silsesquioxanes (POSS) embedded into PEBA 1657 or PEBA 2533	Prediction of transport and structural behaviour and properties of PEG functionalized POSS dispersed in both polyether block amide namely PEBA 1657 and PEBA 2533 using molecular dynamic simulation.	- Simulation method: MD and Monte Carlo - Software: Materials Studio - Forcefield: COMPASS	Gas separation	PEBA 1657 +30% PEG functionalized POSS performance is the closest to the Robeson upper bound with CO ₂ permeability of 100 Barrer and CO ₂ /CH ₄ selectivity of 70.	Simulated T_g and experimental T_g for both PEBA 1657 and PEBA 2533 has percent error of <5%
(Ahmad et al., 2018)	-NH ₂ and -NH-COCH ₃ functionalized metal organic frameworks (MOFs) in 6FDA-DAM polymer MOF used: UiO-66 (Zr-BDC)	Evaluation of the functionalized MOF/6FDA-DAM separation performance and pristine 6FDA-DAM performance.	- Simulation method: MD - Software: LAMMPS - Forcefield: AMBER	Gas separation for CO ₂ /CH ₄	Best separation performance membrane: 14 wt% UiO-66 MMM ($P_{CO_2} = 1912 \pm 115$ Barrer, $\alpha_{CO_2/CH_4} = 31 \pm 1$) 16 wt% UiO-66-NH ₂ MMM ($P_{CO_2} = 1223 \pm 123$ Barrer, $\alpha_{CO_2/CH_4} = 30 \pm 1$)	
(Mosadegh et al., 2020)	Sulfonic acid or amine functionalized-faujasite/poly(ether-block-amide) FAU/PEBA(P8) P8 is PEBA membrane with 8% concentration.	The author functionalized zeolite FAU with sulfonic acid and amine for incorporation to PEBA. The structural properties and transport behaviour are investigated using molecular modelling.	- Simulation method: MD and GCMC - Software: Materials Studio	Gas separation for CO ₂ /CH ₄	P8FAU-NH ₂ (1 wt%) has the highest ideal CO ₂ /CH ₄ selectivity of 45 and permeability of 9 Barrer at 3.48 (1000/T, K ⁻¹)	Simulation data and experimental data has percent error of <5%.
(Liu et al., 2021)	Hollow silica Porous liquid (SPL) functionalize into Pebax-1657 matrix.	Applied Molecular Simulation to verify the improved interaction of the functionalized MMM and CO ₂ molecules by analyzing the interaction parameters including the transport properties.	Simulation method: GCMC	Gas separation for CO ₂ /N ₂	The functionalized MMM gives: CO ₂ permeability up to 229.5 Barrer CO ₂ /N ₂ selectivity of 71.1	Experimental and modelled both exhibit good permeability with percent error of <5%.

530 all gas permeates through the carbon nanotubes in SWCNT's diffusive tunnels and the dispersion of nanotubes in the
531 polymer matrix are well dispersed (Kim et al., 2007). However, at higher SWCNT loadings (15 wt%), the tortuosity
532 throughout the agglomerated SWCNT domains restricts further permeability. Also, there is an observed decrease in
533 CH_4/H_2 experimental selectivity which conforms with CH_4/H_2 selectivities in SWCNTs as predicted by atomistic
534 simulation. Addition of functionalized SWNTs to PSF matrix improve the selectivities and permeabilities of smaller
535 molecules.

537 Incorporation of 11.25 wt% OAPS into the PI polymer matrix exhibit an increase of T_g while a decrease of the T_g
538 is observed when OHS is incorporated into the PI matrix (Yani and Lamm, 2009). Through RDF calculations, it is
539 found that the PI-OHS contacts' density is higher than PI-OAPS contacts' density. PI chains are more closely packed
540 around OHS than OAPS. OHS molecules are positioned in a more orderly manner than OAPS molecules in the
541 nanocomposite membranes. Introduction of OAPS reduced the PI mobility while OHS slightly increased the PI chains
542 mobility.

543 The molar and FFVs decreased with decreasing AAIL size, enabling increased carbon dioxide adsorption and
544 decreased N_2 absorption (Kasahara et al., 2016). It was found that the more the number of amino groups in the AAILs,
545 the CO_2 absorption increase. Multi-amino functionalized AAILs are suitable under humid condition as water
546 molecules aids CO_2 absorption by the AAILs' second amino group.

547 The solubility parameter of pristine MWCNT and P84 shows the largest variance in value between all CNTs and
548 P84, which may indicate poor affinity towards each other (Park et al., 2016). Experimental results confirmed that P84
549 and non-functionalized MWCNT do not mix well and have low mutual compatibility. However, functionalized
550 MWCNTs and P84 have similar solubility parameters, indicating better miscibility and dispersion of functionalized
551 MWCNT in P84 polymer matrix and validated with experimental data. The functional groups must be embedded into
552 the MWCNTs model (with limitation of 0.5-1.0 wt% concentration) for good dispersion through the P84 matrix. If
553 functional groups exceed limit of 1 wt%, the model will show strong phase separation. The number of functional
554 groups shall not exceed a specific limit, else the apolar-polar repulsion between polar heads and carbon together with
555 polar-polar and apolar-apolar interactions occur resulting in phase separation.

556 Improvement of the transport properties including permeability, diffusivity and solubility is observed with the
557 incorporation of either pristine CNT or PEG-functionalized CNT particles up to 2 wt% into the PIM-1 membranes,
558 without compromising on the selectivity, and starts to decrease beyond 2 wt%, while selectivity remains the same
559 (Golzar et al., 2017b). PIM-1/*f*-SWCNT membrane gives the highest diffusivity and permeability; PIM-1/*f*-MWCNT

560 gives the highest CO₂ selectivity. It is found that the resulting nanocomposite (up to 2 wt%) contains polar
561 hydroxyl group that have affinity for the adsorption of quadrupolar CO₂ gas, beyond 2 wt% there is a discontinuity of
562 nano gaps due to agglomeration of the CNTs imposing resistance of diffusing gas through the membrane.

563 Membranes with PEBA 2533 shows higher permeability as compared to PEBA 1657 although results showed
564 otherwise for permselectivity (Pazirofteh et al., 2017). The T_g for POSS-PEG/PEBA 1657 and POSS-PEG/PEBA
565 2533 membranes decreased with the increase of POSS-PEG nanoparticle content. The incorporation of nanomaterial
566 increases the free volume and polymer chain flexibility.

567 Functionalized UiO-66 with 20 wt% of UiO-66-NH₂ and UiO-66-NH-COCH₃ observed improvements in both
568 CO₂ permeability and CO₂/CH₄ selectivity contributed by the decreased T_g and FFV increment due to the disruption
569 to the polymer chain packing (Ahmad et al., 2018).

570 According to M. Mosadegh et. al. (2020), the blending of sulfonic acid or amine functionalized FAU fillers to P8
571 interrupted the P8 polymer chains which increase the FFV, improving the gas diffusion. Improved adsorption and the
572 transportation of gas molecules is facilitated due to the polar groups' presence on the surface of FAU. Amine-FAU/P8
573 (1 wt% amine) gives better performance for CO₂/N₂ selectivity of 117, while SO₃-FAU/P8 (1 wt% SO₃) gives higher
574 CO₂/CH₄ selectivity of 31 (Mosadegh et al., 2020).

575 The as prepared hollow silica-based porous liquids functionalized Pebax-1657 has shown increment of 241.9%
576 of CO₂ permeability and increment of 90.2% of CO₂/N₂ selectivity as compared to the pure Pebax-1657 (Liu et al.,
577 2021). The SPL disrupted Pebax chain arrangement, and the hollow cavity of the porous liquid serves as a pathway
578 for gas transport. The CO₂-philic moieties derived from the porous liquid leads to improved CO₂ selective permeation,
579 overcoming the 2008 Robeson upper bound.

580 Computed FHM exhibits superior results and tailored to its application. During computation of FHM, it is found
581 that functionalized components of the membrane modify the membrane structure where the cavity and pore size are
582 suited to the desired molecular sizes for permeation and retention of respective contaminant molecules, modify the
583 membrane polarity or modify the membrane contaminant-philicity (Yani and Lamm, 2009; Park et al., 2016; Liu et
584 al., 2021).

585 A number of molecular simulation works have reported on the use functionalization of CNTs (Kim et al., 2007;
586 Park et al., 2016; Golzar et al., 2017a) mainly due to its high surface area and good material properties, such as high
587 mechanical strength and good thermal conductivity (Singh et al., 2016). The base polymer material may exhibit
588 reduced mobility when incorporated with functionalized inorganic compound (Yani and Lamm, 2009). Thus, polymer
589 with flexible backbone can be considered for application in future studies.

besides solution-diffusion mechanism. Sulfonate or amine functionalized hybrid membrane can increase the membrane's polarity and its affinity for CO₂ (Kasahara et al., 2016; Mosadegh et al., 2020). PEG functional groups exhibit high permeability without compromising on the selectivity of the hybrid membrane (Golzar et al., 2017a; Pazirofteh et al., 2017).

A few researchers have focused the computation of FHM on gas separation for CO₂ from mainly CH₄. Only one has reported on the computation of FHM for water treatment (Park et al., 2016). The limited number of studies indicates that this section might still be new. This observation suggests more studies are warranted to understand its value and create deeper insight on FHM. The simulation work is also in very small/microscopic scale. It lacks macroscopic representation of the actual scale application and the separation performance in aggressive environment, large scale and the long-term application is not known. The FHM are also normally assumed homogeneous if they have similar or T_g that are near.

Table 4 shows the available data for the enhancement of hybrid membranes from the research work collected from Table 1, 2 and 3.

Table 4 Tabulation of performance enhancement between the pristine membrane and hybrid membrane

Reference	Parameter	Pristine membrane	Hybrid Membrane	Improvement (Folds)
Ionic Liquid Membrane				
(Abedini et al., 2017)	CO ₂ solubility, mol/(L.atm)	0.075	0.066	0.88
(Budhathoki et al., 2017)	CO ₂ solubility, mol fraction	0.025	0.075	3
(Ying et al., 2018)	CO ₂ permeance, GPU	17	68.5	4.03
(Zeng et al., 2018)	CO ₂ loading, mol/kg	3.75	5.5	1.47
(Szala-Bilnik et al., 2019)	CO ₂ MSD (x 10 ⁻⁹ cm ² s ⁻¹)	2.3	7.63	3.32
(Tang et al., 2019)	Butanol Adsorption, nmol/g	0.39	2.83	7.25
(Rahmani et al., 2020)	CO ₂ Diffusivity (x 10 ⁻¹¹ m ² /s)	2.8	6	2.14
(Ishak et al., 2020)	CO ₂ Diffusivity, nm ² /ps	397.183	60.067	0.15
(You et al., 2022)	CO ₂ Diffusion coefficient (x 10 ⁻¹¹ m ² s ⁻¹)	130	120	0.91
Mixed Matrix Membrane				
(Golzar et al., 2014)	CO ₂ Permselectivity	25.3	23.2	0.92
(Dehghani et al., 2017)	CO ₂ Permselectivity	20.11	57.83	2.88
(Kong and Liu, 2019)	CO ₂ Diffusivity (x 10 ⁻⁹ m ² /s)	0.12	0.15	1.25

Reference	Parameter	Pristine membrane	Hybrid Membrane	Improvement (Folds)
(Liu et al., 2019a)	CO ₂ permeability (Barrer)	46	67	1.46
(Riasat Harami et al., 2019)	CO ₂ solubility	33.1	11.32	0.34
(Amirkhani et al., 2020)	CO ₂ Permselectivity	25.7	29.13	1.13
(Mosadegh et al., 2020)	CO ₂ permeability (Barrer)	70	110	1.57
(Riasat Harami et al., 2020)	CO ₂ permeability (Barrer)	7.21	4.05	0.56
(Wei et al., 2020)	Water permeability (x 10 ⁻⁷ L.m/(h.m ² .bar))	3.3	4.5	1.36
(Salahshoori et al., 2021a)	CO ₂ Permeability (Barrer)	7.9	14.76	1.87
Functionalized Hybrid Membrane				
(Kim et al., 2007)	Permeability (Barrer)	3.9	5.19	1.33
(Pazirofteh et al., 2017)	Permselectivity	1	1	1
(Ahmad et al., 2018)	Permeability (Barrer)	997	1912	1.92
(Liu et al., 2021)	Permeability (Barrer)	70	229.4	3.28

605

606

607

608

609

610

611

4. CONCLUSIONS AND FUTURE PERSPECTIVES

612

613

614

615

616

617

618

619

620

621

In conclusion, molecular simulation approaches aid to unravel molecule interactions with the environment and complex materials in complementary to experiments. Although the computational method may become more heavily dependent upon in the future, the Molecular Dynamics-based prediction process is still a complicated and challenging task. Precise data input and sufficient timescale must be provided to converge the simulation into more reliable and accurate outcomes. It was observed from the review that via proper design and selection of ionic liquid, inorganic material or functionalized material using molecular simulation, the separation performance of polymeric membrane can be enhanced by a few times ranging from two to four folds. Functionalized hybrid membranes are observed to have better overall improvement in separation performance, while ionic liquid membranes and mixed matrix membranes have a combination of enhanced and deteriorated performance compared to its pristine membrane. This finding highlights the importance of elucidation of suitable hybrid membrane material and its gas transport properties

622 by ~~membrane modification, a potential solution to reduce time-consuming experiments due to trial and error for making~~ ing
623 new hybrid membrane materials in the laboratory for various application (Smith and Qi, 2018).

624 A comprehensive molecular simulation along with justifications from theoretical calculations can provide
625 researchers with vast details and parameters of the system. This can lead to the design and development of tailor-made
626 and engineered materials at the most optimum separation. Hence, molecular simulation is expected to continuously
627 contribute to the testing of new applications for various fields such as sour gas removal in the energy sector to reduce
628 global warming, water and wastewater treatment to protect human from harmful element in water, water desalination
629 which is a solution to source for fresh water for industrial/domestic use and human consumption, and etc. In particular,
630 the removal of CO₂ is important in reducing the concentration in the atmosphere responsible for global warming and
631 wastewater treatment could protect human from harmful elements found in water and ensure maximum amount of
632 water to be reused especially in places with limited freshwater source.

633 Based on the recent advances in molecular simulation, the followings are the aspects that would gain attraction in
634 the research and development of molecular simulations.

635 636 **4.1 Innovative Membrane Modifications and Combinations**

637 The explorations of new membrane materials are required for new applications. Although membrane
638 modifications will find their niche in terms of small-scale development, there may be limitations during large scale
639 production of the membranes. More molecular simulation research is required to interpret the roles of new materials
640 in the membrane structure, morphology, and effect on solute transport.

641 Studying the safety and environmental aspects of the membrane modification will be beneficial for real life
642 applications. Careful selection of materials should be given for tailor-made modified membranes that are important
643 for enhancement in the aspects of selectivity, diffusivity, and intrinsic properties. This will lead to breakthrough in
644 optimizing membrane performance.

645 646 **4.2 Environmental Aspects**

647 The inevitable large-scale applications and non-scientific disposal of membrane materials pose severe threat to
648 environments, especially those non-biodegradable membranes with polymer base made of ethylene, polycarbonate,
649 polystyrene, polyvinyl chloride, polypropylene, and polyester. Future direction of membrane industries should
650 emphasize on the development of sustainable polymer in an economical manner. This can be achieved with

651 tra... may
652 serve as the starting gate to explore new materials that are environmentally friendly and practical for application.
653

654 **4.3 Long Term Techno-Economic Studies of Membrane Advancement Application**

655 Although many improvements can be observed from the advancement of membrane technology, the diversity and
656 operating range of actual large-scale membrane-based separation remains limited. The separation performance of the
657 membrane materials in aggressive actual conditions is unknown despite proven to improve separation and mechanical
658 strength performance in simulations. These materials are highly attractive for future considerations due to their
659 advantages of portable and easy maintenance.

660 A number of studies have reported new and interesting applications with membrane advancement in many areas
661 in small scale but none have reported on the large scale and long-term operation of the processes (Fu et al., 2021;
662 Jiang et al., 2021; Moqadam et al., 2021; Zhang et al., 2021). The technical barriers in molecular modelling include
663 membrane physical aging, fillers, and ionic liquid having plasticization effect to the membrane. In addition, multiscale
664 modelling for system description and hybrid membrane homogeneity are normally presumed to be homogenous.
665 These challenges shall be addressed to achieve a more reliable modelling outcome.

666 For the membrane operation to perform, techno-economic assessment of the process at pilot scale is necessary.
667 This will resolve many issues like the viability, profitability, swelling control and mitigation, and the membrane
668 susceptibility to complex feed materials. Such studies are costly and time-consuming, but successful outcomes will
669 lead to a more sustainable membrane separation operation. Solitary membrane process may not be able to perform
670 well, but the overall process can be improved when incorporated with filler or ionic liquid.

671 Reliable simulation and modelling can be used to predict the performance of the new hybrid membrane in which
672 it can provide guidelines on the operating conditions of the process. This reduces the amount of time in conducting
673 the experimental study. A new way of bringing the advancement of membrane separation technology to real-life
674 applications is highly promising for the decades to come.

676 **Funding**

677 This work is done with the financial support from Yayasan Universiti Teknologi PETRONAS (Grant No: 015LC0-
678 322).

680 **Conflicts of Interest**

There are no comments to be made.

Acknowledgement

The technical support provided by CO₂ Research Centre (CO₂RES) research group, Universiti Teknologi PETRONAS, is duly acknowledged.

Authorship contribution statement

Cia Yin Yee - Original draft; Data curation; Formal analysis; Investigation, Lam Ghai Lim - Formal analysis; Writing – review & editing; Investigation, Serene Sow Mun Lock – Formal analysis; Supervision; Writing – review & editing; Investigation, Norwahyu Jusoh – Resources; Writing – review & editing; Chung Loong Yiin – Resources; Writing – review & editing; Bridgid Lai Fui Chin – Resources; Writing – review & editing; Yi Heng Chan – Resources; Writing – review & editing; Adrian Chun Minh Loy – Resources; Writing – review & editing; Muhammad Mubashir – Resources; Writing – review & editing

5. REFERENCES

- Abedini, A., Crabtree, E., Bara, J.E., Turner, C.H., 2017. Molecular Simulation of Ionic Polyimides and Composites with Ionic Liquids as Gas-Separation Membranes. *Langmuir* 33, 11377-11389.
- Adams, R., Lee, J., Bae, T.-H., Ward, J., Johnson, J.R., Jones, C., Nair, S., Koros, W., 2011. CO₂-CH₄ permeation in high zeolite 4A loading mixed matrix membranes. *Fuel and Energy Abstracts* 367, 197-203.
- Adcock, S.A., McCammon, J.A., 2006. Molecular Dynamics: Survey of Methods for Simulating the Activity of Proteins. *Chemical Reviews* 106, 1589-1615.
- Ahmad, A., Waheed, S., Khan, S.M., e-Gul, S., Shafiq, M., Farooq, M., Sanaullah, K., Jamil, T., 2015. Effect of silica on the properties of cellulose acetate/polyethylene glycol membranes for reverse osmosis. *Desalination* 355, 1-10.
- Ahmad, M.Z., Navarro, M., Lhotka, M., Zornoza, B., Téllez, C., de Vos, W.M., Benes, N.E., Konnertz, N.M., Visser, T., Semino, R., Maurin, G., Fila, V., Coronas, J., 2018. Enhanced gas separation performance of 6FDA-DAM based mixed matrix membranes by incorporating MOF UiO-66 and its derivatives. *Journal of Membrane Science* 558, 64-77.
- Alavi, S., 2020. *Molecular Simulations: Fundamentals and Practice*. Wiley.
- Alves, E.D., Oliveira, L.B.A., Colherinhas, G., 2019. Understanding the stability of polypeptide membranes in ionic liquids: a theoretical molecular dynamics study. *New Journal of Chemistry* 43, 10151-10161.
- Amirkhani, F., Harami, H.R., Asghari, M., 2020. CO₂/CH₄ mixed gas separation using poly(ether-b-amide)-ZnO nanocomposite membranes: Experimental and molecular dynamics study. *Polymer Testing* 86, 106464.
- An, Y., Fu, Q., Zhang, D., Wang, Y., Tang, Z., 2019. Performance evaluation of activated carbon with different pore sizes and functional groups for VOC adsorption by molecular simulation. *Chemosphere* 227, 9-16.
- Asche, T.S., Behrens, P., Schneider, A.M., 2017. Validation of the COMPASS force field for complex inorganic-organic hybrid polymers. *Journal of Sol-Gel Science and Technology* 81, 195-204.
- Asif, K., Lock, S.S.M., Taqvi, S.A.A., Jusoh, N., Yiin, C.L., Chin, B.L.F., Loy, A.C.M., 2021. A Molecular Simulation Study of Silica/Polysulfone Mixed Matrix Membrane for Mixed Gas Separation. *Polymers* 13, 2199.
- Bouzd, L., Hiadsi, S., Bensaid, M.O., Foudad, F.Z., 2018. Molecular dynamics simulation studies of the miscibility and thermal properties of PMMA/PS polymer blend. *Chinese Journal of Physics* 56, 3012-3019.
- Brunetti, A., Macedonio, F., Barbieri, G., Drioli, E., 2015. Membrane engineering for environmental protection and sustainable industrial growth: Options for water and gas treatment. *Environmental Engineering Research* 20, 307-328.
- Budhathoki, S., Shah, J.K., Maginn, E.J., 2017. Molecular Simulation Study of the Performance of Supported Ionic Liquid Phase Materials for the Separation of Carbon Dioxide from Methane and Hydrogen. *Industrial & Engineering Chemistry Research* 56, 6775-6784.

- 726 Cai, W., Li, S., Li, C., 2021. *Molecular Dynamics Simulations*, Ninth (ed.), Comprehensive Nuclear Materials.
727 Elsevier, Oxford, pp. 249-265.
- 728 Chen, Y., Teng, J., Liao, B.-Q., Li, R., Lin, H., 2020. Molecular insights into the impacts of iron(III) ions on membrane
729 fouling by alginate. *Chemosphere* 242, 125232.
- 730 Cheng, Y., Guo, Y., He, H., Ding, W., Diao, Y., Huo, F., 2021. Mechanistic Understanding of CO₂ Adsorption and
731 Diffusion in the Imidazole Ionic Liquid–Hexafluoroisopropylidene Polyimide Composite Membrane. *Industrial &
732 Engineering Chemistry Research* 60, 6027-6037.
- 733 Cornell, W.D., Cieplak, P., Bayly, C.I., Gould, I.R., Merz, K.M., Ferguson, D.M., Spellmeyer, D.C., Fox, T., Caldwell, J.W.,
734 Kollman, P.A., 1995. A Second Generation Force Field for the Simulation of Proteins, Nucleic Acids, and Organic
735 Molecules. *Journal of the American Chemical Society* 117, 5179-5197.
- 736 Corti, D., 2002. Monte Carlo simulations in the isothermal-isobaric ensemble: The requirement of a 'shell' molecule
737 and simulations of small systems. *Molecular Physics* 100, 1887-1904.
- 738 Dehghani, M., Asghari, M., Ismail, A.F., Mohammadi, A.H., 2017. Molecular dynamics and Monte Carlo simulation of
739 the structural properties, diffusion and adsorption of poly (amide-6-b-ethylene oxide)/Faujasite mixed matrix
740 membranes. *Journal of Molecular Liquids* 242, 404-415.
- 741 Deqian, R., 1987. Cleaning and Regeneration of Membranes. *Desalination* 62, 363-371.
- 742 Ebrahim, S., 1994. Cleaning and regeneration of membranes in desalination and wastewater applications: State-of-
743 the-art. *Desalination* 96, 225-238.
- 744 Ebro, H., Kim, Y.M., Kim, J.H., 2013. Molecular dynamics simulations in membrane-based water treatment processes:
745 A systematic overview. *Journal of Membrane Science* 438, 112–125.
- 746 Einstein, A., Schilpp, P.A., 1979. *Autobiographical notes*.
- 747 Freeman, B.D., 1999. Basis of Permeability/Selectivity Tradeoff Relations in Polymeric Gas Separation Membranes.
748 *Macromolecules* 32, 375-380.
- 749 Fu, L., Yang, Z., Wang, Y., Li, R., Zhai, J., 2021. Construction of Metal–Organic Frameworks (MOFs)–Based Membranes
750 and Their Ion Transport Applications. *Small Science* 1, 2000035.
- 751 Gokulakrishnan, S.A., Arthanareeswaran, G., László, Z., Veréb, G., Kertész, S., Kweon, J., 2021. Recent development
752 of photocatalytic nanomaterials in mixed matrix membrane for emerging pollutants and fouling control, membrane
753 cleaning process. *Chemosphere* 281, 130891.
- 754 Golzar, K., Amjad-Iranagh, S., Amani, M., Modarress, H., 2014. Molecular simulation study of penetrant gas transport
755 properties into the pure and nanosized silica particles filled polysulfone membranes. *Journal of Membrane Science*
756 451, 117-134.
- 757 Golzar, K., Modarress, H., Amjad-Iranagh, S., 2017a. Effect of pristine and functionalized single- and multi-walled
758 carbon nanotubes on CO₂ separation of mixed matrix membranes based on polymers of intrinsic microporosity
759 (PIM-1): a molecular dynamics simulation study. *Journal of Molecular Modeling* 23, 266.
- 760 Golzar, K., Modarress, H., Amjad-Iranagh, S., 2017b. Separation of gases by using pristine, composite and
761 nanocomposite polymeric membranes: A molecular dynamics simulation study. *Journal of Membrane Science* 539,
762 238-256.
- 763 Gonzalez-Miquel, M., Palomar, J., Omar, S., Rodriguez, F., 2011. CO₂/N₂ Selectivity Prediction in Supported Ionic
764 Liquid Membranes (SILMs) by COSMO-RS. *Industrial & Engineering Chemistry Research* 50, 5739-5748.
- 765 He, Z., Kumar Reddy, K.S., Karanikolos, G., Wang, K., 2018. Chapter 5 - CO₂/CH₄ Separation (Natural Gas Purification)
766 by Using Mixed Matrix Membranes. in: Basile, A., Favvas, E.P. (Eds.). *Current Trends and Future Developments on
767 (Bio-) Membranes*. Elsevier, pp. 155-181.
- 768 Hernández-Rodríguez, M., Rosales-Hernández, M., Mendieta-Wejebe, J., Martínez-Archundia, M., Correa-Basurto,
769 J., 2016. Current Tools and Methods in Molecular Dynamics (MD) Simulations for Drug Design. *Current medicinal
770 chemistry* 23.
- 771 Hollingsworth, S.A., Dror, R.O., 2018. Molecular Dynamics Simulation for All. *Neuron* 99, 1129-1143.
- 772 Hwang, S., Semino, R., Seoane, B., Zahan, M., Chmelik, C., Valiullin, R., Bertmer, M., Haase, J., Kapteijn, F., Gascon,
773 J., Maurin, G., Kärger, J., 2018. Revealing Transient Concentration of CO₂ in a Mixed Matrix Membrane by IR
774 Microimaging and Molecular Modeling. *Angewandte Chemie* 130.
- 775 Ishak, M.A.I., Jumbri, K., Daud, S., Abdul Rahman, M.B., Abdul Wahab, R., Yamagishi, H., Yamamoto, Y., 2020.
776 Molecular simulation on the stability and adsorption properties of choline-based ionic liquids/IRMOF-1 hybrid
777 composite for selective H₂S/CO₂ capture. *Journal of Hazardous Materials* 399, 123008.
- 778 Jiang, K., Zhou, G., Fang, T., Liu, X., 2021. Permeability of vesicles for imidazolium-based ionic liquids in aqueous
779 solution: a molecular dynamic simulation study. *Industrial & Engineering Chemistry Research* 60, 3174-3183.

- Jiang, H., Deng, H., Li, H., Wang, H., Li, H., Li, H., Li, H., 2020. Effect of copper nanoparticles on thermal behavior of water flow in a zig-zag nanochannel using molecular dynamics simulation. *International Communications in Heat and Mass Transfer* 116, 104652.
- Jusoh, N., Yeong, Y.F., Chew, T.L., Lau, K.K., Shariff, A.M., 2016. Current Development and Challenges of Mixed Matrix Membranes for CO₂/CH₄ Separation. *Separation & Purification Reviews* 45, 321-344.
- Kasahara, S., Kamio, E., Shaikh, A.R., Matsuki, T., Matsuyama, H., 2016. Effect of the amino-group densities of functionalized ionic liquids on the facilitated transport properties for CO₂ separation. *Journal of Membrane Science* 503, 148-157.
- Keskin, S., 2010. Molecular Simulation Study of CH₄/H₂ Mixture Separations Using Metal Organic Framework Membranes and Composites. *The Journal of Physical Chemistry C* 114, 13047-13054.
- Keskin, S., Alsoy Altinkaya, S., 2019. A Review on Computational Modeling Tools for MOF-Based Mixed Matrix Membranes. *Computation* 7, 36.
- Kim, S., Chen, L., Johnson, J.K., Marand, E., 2007. Polysulfone and functionalized carbon nanotube mixed matrix membranes for gas separation: Theory and experiment. *Journal of Membrane Science* 294, 147-158.
- Kong, X., Liu, J., 2019. An Atomistic Simulation Study on POC/PIM Mixed-Matrix Membranes for Gas Separation. *The Journal of Physical Chemistry C* 123, 15113-15121.
- Krishna, R., van Baten, J.M., 2010. In silico screening of zeolite membranes for CO₂ capture. *Journal of Membrane Science* 360, 323-333.
- Le, N.L., Nunes, S.P., 2016. Materials and membrane technologies for water and energy sustainability. *Sustainable Materials and Technologies* 7, 1-28.
- Lee, B.-Y., Park, S., Chung, D.-W., Jang, K.-S., 2022. Incorporation of alkyl-functionalized silica nanoparticles into hydrophilic epoxy and hydrophobic polystyrene matrices. *Journal of Applied Polymer Science* 139, 51828.
- Liguori, S., Wilcox, J., 2018. Chapter 14 - Design Considerations for Postcombustion CO₂ Capture With Membranes. in: Basile, A., Favvas, E.P. (Eds.). *Current Trends and Future Developments on (Bio-) Membranes*. Elsevier, pp. 385-413.
- Liu, J., Xu, Q., Jiang, J., 2019a. A molecular simulation protocol for swelling and organic solvent nanofiltration of polymer membranes. *Journal of Membrane Science* 573, 639-646.
- Liu, S., Meng, L., Fan, J., 2021. Hollow Silica-Based Porous Liquids Functionalized Mixed Matrix Membranes for CO₂ Capture. *ChemistrySelect* 6, 5027-5033.
- Liu, Y.-C., Chen, C.-Y., Lin, G.-S., Chen, C.-H., Wu, K.C.W., Lin, C.-H., Tung, K.-L., 2019b. Characterization and molecular simulation of Pebax-1657-based mixed matrix membranes incorporating MoS₂ nanosheets for carbon dioxide capture enhancement. *Journal of Membrane Science* 582, 358-366.
- Lock, S.S.M., Lau, K.K., Shariff, A.M., Yeong, Y.F., Bustam, M.A., Jusoh, N., Ahmad, F., 2018. An atomistic simulation towards elucidation of operating temperature effect in CO₂ swelling of polysulfone polymeric membranes. *Journal of Natural Gas Science and Engineering* 57, 135-154.
- Lock, S.s.M., Yiin, C.L., 2020. An atomistic simulation towards molecular design of silica polymorphs nanoparticles in polysulfone based mixed matrix membranes for CO₂/CH₄ gas separation. *Polymer Engineering & Science* 60.
- Manikandan, S., Subbaiya, R., Saravanan, M., Ponraj, M., Selvam, M., Pugazhendhi, A., 2022. A critical review of advanced nanotechnology and hybrid membrane based water recycling, reuse, and wastewater treatment processes. *Chemosphere* 289, 132867.
- McCarthy, C., Vaughan, T., 2015. 14 - Micromechanical failure analysis of advanced composite materials. in: Camanho, P.P., Hallett, S.R. (Eds.). *Numerical Modelling of Failure in Advanced Composite Materials*. Woodhead Publishing, pp. 379-409.
- Mehana, M., Kang, Q., Nasrabadi, H., Viswanathan, H., 2021. Molecular Modeling of Subsurface Phenomena Related to Petroleum Engineering. *Energy Fuels* 35, 2851-2869.
- Mohammadi, M., Asadollahzadeh, M., Shirazian, S., 2018. Molecular-level understanding of supported ionic liquid membranes for gas separation. *Journal of Molecular Liquids* 262, 230-236.
- Mollahosseini, A., Abdelrasoul, A., 2021. Molecular dynamics simulation for membrane separation and porous materials: A current state of art review. *Journal of Molecular Graphics and Modelling* 107, 107947.
- Monsalve-Bravo, G.M., Dutta, R.C., Bhatia, S.K., 2020. Multiscale simulation of gas transport in mixed-matrix membranes with interfacial polymer rigidification. *Microporous and Mesoporous Materials* 296, 109982.
- Moqadam, M., Tubiana, T., Moutoussamy, E.E., Reuter, N., 2021. Membrane models for molecular simulations of peripheral membrane proteins. *Advances in Physics: X* 6, 1932589.

- 833 Mousalegh, M., Aminian, H., Mousa Harami, H., Roghani, M., Farmani, M., 2020. Effect of Nitric and Ph-POSS
834 functionalization on mixed gas separation of PEBA-FAU membranes: Experimental study and MD and GCMC
835 simulations. *Separation and Purification Technology* 247, 116981.
- 836 Murzyn, K., Bratek, M., Pasenkiewicz-Gierula, M., 2013. Refined OPLS All-Atom Force Field Parameters for n-
837 Pentadecane, Methyl Acetate, and Dimethyl Phosphate. *The Journal of Physical Chemistry B* 117, 16388-16396.
- 838 Najafi, M., Sadeghi, M., Bolverdi, A., Pourafshari Chenar, M., Pakizeh, M., 2018. Gas permeation properties of
839 cellulose acetate/silica nanocomposite membrane. *Advances in Polymer Technology* 37, 2043-2052.
- 840 Park, C.H., Tocci, E., Fontananova, E., Bahattab, M.A., Aljlil, S.A., Drioli, E., 2016. Mixed matrix membranes containing
841 functionalized multiwalled carbon nanotubes: Mesoscale simulation and experimental approach for optimizing
842 dispersion. *Journal of Membrane Science* 514, 195-209.
- 843 Pazirofteh, M., Dehghani, M., Niazi, S., Mohammadi, A.H., Asghari, M., 2017. Molecular dynamics simulation and
844 Monte Carlo study of transport and structural properties of PEBA 1657 and 2533 membranes modified by
845 functionalized POSS-PEG material. *Journal of Molecular Liquids* 241, 646-653.
- 846 Qian, Q., Asinger, P.A., Lee, M.J., Han, G., Mizrahi Rodriguez, K., Lin, S., Benedetti, F.M., Wu, A.X., Chi, W.S., Smith,
847 Z.P., 2020. MOF-Based Membranes for Gas Separations. *Chemical Reviews* 120, 8161-8266.
- 848 Rackley, S.A., 2017. 8 - Membrane separation systems. in: Rackley, S.A. (Ed.). *Carbon Capture and Storage (Second
849 Edition)*. Butterworth-Heinemann, Boston, pp. 187-225.
- 850 Rahmani, F., Nouranian, S., Chiew, Y.C., 2020. 3D Graphene as an Unconventional Support Material for Ionic Liquid
851 Membranes: Computational Insights into Gas Separations. *Industrial & Engineering Chemistry Research* 59, 2203-
852 2210.
- 853 Riasat Harami, H., Dashti, A., Ghahramani Pirsalami, P., Bhatia, S.K., Ismail, A.F., Goh, P.S., 2020. Molecular
854 Simulation and Computational Modeling of Gas Separation through Polycarbonate/p-Nitroaniline/Zeolite 4A Mixed
855 Matrix Membranes. *Industrial & Engineering Chemistry Research* 59, 16772-16785.
- 856 Riasat Harami, H., Riazi Fini, F., Rezakazemi, M., Shirazian, S., 2019. Sorption in mixed matrix membranes:
857 Experimental and molecular dynamic simulation and Grand Canonical Monte Carlo method. *Journal of Molecular
858 Liquids* 282, 566-576.
- 859 Rindt, C.C.M., Gaastra-Nedea, S.V., 2015. 15 - Modeling thermochemical reactions in thermal energy storage
860 systems. in: Cabeza, L.F. (Ed.). *Advances in Thermal Energy Storage Systems*. Woodhead Publishing, pp. 375-415.
- 861 Salahshoori, I., Nasirian, D., Rashidi, N., Hossain, M.K., Hatami, A., Hassanzadeganroudsari, M., 2021a. The effect of
862 silica nanoparticles on polysulfone-polyethylene glycol (PSF/PEG) composite membrane on gas separation and
863 rheological properties of nanocomposites. *Polymer Bulletin* 78, 3227-3258.
- 864 Salahshoori, I., Seyfaee, A., Babapoor, A., Neville, F., Moreno-atanasio, R., 2021b. Evaluation of the effect of silica
865 nanoparticles, temperature and pressure on the performance of PSF/PEG/SiO₂ mixed matrix membranes: A
866 molecular dynamics simulation (MD) and design of experiments (DOE) study. *Journal of Molecular Liquids* 333,
867 115957.
- 868 Setiawan, W.K., Chiang, K.-Y., 2019. Silica applied as mixed matrix membrane inorganic filler for gas separation: a
869 review. *Sustainable Environment Research* 29, 32.
- 870 Sharma, S.K., Pramod; Chandra, Rakesh, 2019. Chapter 2 - Overview of BIOVIA Materials Studio, LAMMPS, and
871 GROMACS. in: Sharma, S. (Ed.). *Molecular Dynamics Simulation of Nanocomposites Using BIOVIA Materials Studio,
872 Lammps and Gromacs*. Elsevier, pp. 39-100.
- 873 Shirts, R., Burt, S., Johnson, A., 2006. Periodic boundary condition induced breakdown of the equipartition principle
874 and other kinetic effects of finite sample size in classical hard-sphere molecular dynamics simulation. *The Journal of
875 chemical physics* 125, 164102.
- 876 Singh, B., Lohan, S., Sandhu, P.S., Jain, A., Mehta, S.K., 2016. Chapter 15 - Functionalized carbon nanotubes and their
877 promising applications in therapeutics and diagnostics. in: Grumezescu, A.M. (Ed.). *Nanobiomaterials in Medical
878 Imaging*. William Andrew Publishing, pp. 455-478.
- 879 Singh, J.K., Sharma, R.K., Ghosh, P., Kumar, A., Khan, M.L., 2018. Imidazolium Based Ionic Liquids: A Promising Green
880 Solvent for Water Hyacinth Biomass Deconstruction. *Frontiers in Chemistry* 6.
- 881 Singh, R., 2005. Chapter 4 - Hybrid membrane system design and operation. in: Singh, R. (Ed.). *Hybrid Membrane
882 Systems for Water Purification*. Elsevier Science, Amsterdam, pp. 197-242.
- 883 Smith, W.R., Qi, W., 2018. Molecular Simulation of Chemical Reaction Equilibrium by Computationally Efficient Free
884 Energy Minimization. *ACS Central Science* 4, 1185-1193.
- 885 Song, T., Zhang, X., Li, Y., Jiang, K., Zhang, S., Cui, X., Bai, L., 2019. Separation Efficiency of CO₂ in Ionic
886 Liquids/Poly(vinylidene fluoride) Composite Membrane: A Molecular Dynamics Study. *Industrial & Engineering
887 Chemistry Research* 58, 6887-6898.

- 888 Sulastri, N., Sari, S.N., 2020. Imidazolium-based ionic liquid derivatives, synthesis and evaluation of inhibitory effect
889 on mild steel corrosion in hydrochloric acid solution. *Heliyon* 6, e03498.
- 890 Swati, I.K., Sohaib, Q., Cao, S., Younas, M., Liu, D., Gui, J., Rezakazemi, M., 2021. Protic/aprotic ionic liquids for
891 effective CO₂ separation using supported ionic liquid membrane. *Chemosphere* 267, 128894.
- 892 Szala-Bilnik, J., Abedini, A., Crabtree, E., Bara, J.E., Turner, C.H., 2019. Molecular Transport Behavior of CO₂ in Ionic
893 Polyimides and Ionic Liquid Composite Membrane Materials. *The Journal of Physical Chemistry B* 123, 7455-7463.
- 894 Tahir, Z., Ilyas, A., Li, X., Bilad, M.R., Vankelecom, I.F.J., Khan, A.L., 2018. Tuning the gas separation performance of
895 fluorinated and sulfonated PEEK membranes by incorporation of zeolite 4A. *Journal of Applied Polymer Science* 135,
896 45952.
- 897 Tan, P.C., Ooi, B., Ahmad, A.L., Low, S.C., 2018. Formation of Defect-free Polyimide/Zeoilic Imidazolate Framework-
898 8 Composite Membrane for Gas Separation: In-depth Analysis of Organic-Inorganic Compatibility. *Journal of*
899 *Chemical Technology & Biotechnology* 94.
- 900 Tang, W., Lou, H., Li, Y., Kong, X., Wu, Y., Gu, X., 2019. Ionic liquid modified graphene oxide-PEBA mixed matrix
901 membrane for pervaporation of butanol aqueous solutions. *Journal of Membrane Science* 581, 93-104.
- 902 Theng, S., Jumbri, K., Wirzal, M.D.H., 2017. Molecular dynamics simulation of membrane in room temperature ionic
903 liquids.
- 904 Vara, S., Konni, M., Karnena, M.K., 2020. Membrane Technology for Treatment of Pharmaceutical Wastewaters: A
905 Novel Approach. in: Affam, A.C., Ezechi, E.H. (Eds.). *Handbook of Research on Resource Management for Pollution*
906 *and Waste Treatment*. IGI Global, Hershey, PA, USA, pp. 502-530.
- 907 Vatanpour, V., Pasaoglu, M.E., Barzegar, H., Teber, O.O., Kaya, R., Bastug, M., Khataee, A., Koyuncu, I., 2022.
908 Cellulose acetate in fabrication of polymeric membranes: A review. *Chemosphere* 295, 133914.
- 909 Vergadou, N., Theodorou, D.N., 2019. Molecular Modeling Investigations of Sorption and Diffusion of Small
910 Molecules in Glassy Polymers. *Membranes (Basel)* 9, 98.
- 911 Wang, C., Jagirdar, P., Naserifar, S., Sahimi, M., 2016a. Molecular Simulation Study of Gas Solubility and Diffusion in
912 a Polymer-Boron Nitride Nanotube Composite. *The Journal of Physical Chemistry B* 120, 1273-1284.
- 913 Wang, J., Luo, J., Feng, S., Li, H., Wan, Y., Zhang, X., 2016b. Recent development of ionic liquid membranes. *Green*
914 *Energy & Environment* 1, 43-61.
- 915 Wang, R., Chen, D., Wang, Q., Ying, Y., Gao, W., Xie, L., 2020. Recent Advances in Applications of Carbon Nanotubes
916 for Desalination: A Review. *Nanomaterials* 10, 1203.
- 917 Wei, W., Liu, J., Jiang, J., 2020. Atomistic Simulation Study of Polyarylate/Zeoilic-Imidazolate Framework Mixed-
918 Matrix Membranes for Water Desalination. *ACS Applied Nano Materials* 3, 10022-10031.
- 919 Wong, K.K., Jawad, Z.A., 2019. A review and future prospect of polymer blend mixed matrix membrane for CO₂
920 separation. *Journal of Polymer Research* 26, 289.
- 921 Wu, C., Wang, X., Zhu, T., Li, P., Xia, S., 2020. Covalent organic frameworks embedded membrane via acetic-acid-
922 catalyzed interfacial polymerization for dyes separation: Enhanced permeability and selectivity. *Chemosphere* 261,
923 127580.
- 924 Xu, Q., Jiang, J., 2020. Molecular simulations of liquid separations in polymer membranes. *Current Opinion in*
925 *Chemical Engineering* 28, 66-74.
- 926 Yani, Y., Lamm, M., 2009. Molecular dynamics simulation of mixed matrix nanocomposites containing polyimide and
927 polyhedral oligomeric silsesquioxane (POSS). *Polymer* 50, 1324-1332.
- 928 Ying, W., Cai, J., Zhou, K., Chen, D., Ying, Y., Guo, Y., Kong, X., Xu, Z., Peng, X., 2018. Ionic Liquid Selectively Facilitates
929 CO₂ Transport through Graphene Oxide Membrane. *ACS Nano* 12, 5385-5393.
- 930 You, L., Guo, Y., He, Y., Huo, F., Zeng, S., Li, C., Zhang, X., Zhang, X., 2022. Molecular level understanding of CO₂
931 capture in ionic liquid/polyimide composite membrane. *Frontiers of Chemical Science and Engineering* 16, 141-151.
- 932 Yu, T., Cai, Q., Lian, G., Liu, L., 2022. Molecular dynamics studies on separation of CO₂/CH₄ by the ionic liquids
933 encapsulated ZIF-8. *Journal of Membrane Science* 644, 120117.
- 934 Zeng, Y., Li, K., Zhu, Q., Wang, J., Cao, Y., Lu, S., 2018. Capture of CO₂ in carbon nanotube bundles supported with
935 room-temperature ionic liquids: A molecular simulation study. *Chemical Engineering Science* 192, 94-102.
- 936 Zhang, L., Zhang, M., Liu, G., Jin, W., Li, X., 2021. Fungal cell wall-graphene oxide microcomposite membrane for
937 organic solvent nanofiltration. *Advanced Functional Materials* 31, 2100110.
- 938 Zhao, Z., Jiang, J., 2020. POC/PIM-1 mixed-matrix membranes for water desalination: A molecular simulation study.
939 *Journal of Membrane Science* 608, 118173.
- 940 Zhu, W., Liu, F., Gou, M., Guo, R., Li, X., 2021. Mixed matrix membrane containing metal oxide nanosheets for
941 efficient CO₂ separation. *Green Chemical Engineering* 2, 132-143.

942 Zolghadr, L., Alsaadi, M.S., Alsharadhi, S., Alshaykh, P., Emery, W., 2021. The Role of Membrane based
943 Technologies in Environmental Treatment and Reuse of Produced Water. *Frontiers in Environmental Science* 9.

944

Journal Pre-proof

HIGHLIGHTS

- Fundamentals of molecular simulation are reviewed and related to application in hybrid membranes.
- Insight into molecular structural properties of hybrid membranes is presented.
- Simulated transport performance from published literature and mechanism of hybrid membranes are provided.
- Limitation in molecular simulation for membrane separation is discussed.
- Future outlook for molecular simulation of membrane separation is recommended.

Journal Pre-proof

Declaration of interests

The authors declare that they have no known competing financial interests or personal relationships that could have appeared to influence the work reported in this paper.

The authors declare the following financial interests/personal relationships which may be considered as potential competing interests:

Journal Pre-proof